Active deformation and shallow structure of the Wagner, Consag, and Delfín Basins, northern Gulf of California, Mexico

Patricia Persaud,[1] Joann M. Stock,[1] Michael S. Steckler,[2] Arturo Martín-Barajas,[3] John B. Diebold,[2] Antonio González-Fernández,[3] and Gregory S. Mountain[2]

Received 20 April 2002; revised 3 October 2002; accepted 25 November 2002; published 31 July 2003.

[1] Oblique rifting began synchronously along the length of the Gulf of California at 6 Ma, yet there is no evidence for the existence of oceanic crust or a spreading transform fault system in the northern Gulf. Instead, multichannel seismic data show a broad shallow depression, ~70 × 200 km, marked by active distributed deformation and six ~10-km-wide segmented basins lacking well-defined transform faults. We present detailed images of faulting and magmatism based on the high resolution and quality of these data. The northern Gulf crust contains a dense (up to 18 faults in 5 km) complex network of mainly oblique-normal faults, with small offsets, dips of 60–80° and strikes of N-N30°E. Faults with seafloor offsets of tens of meters bound the Lower and two Upper Delfín Basins. These subparallel basins developed along splays from a transtensional zone at the NW end of the Ballenas Transform Fault. Twelve volcanic knolls were identified and are associated with the strands or horsetails from this zone. A structural connection between the two Upper Delfín Basins is evident in the switching of the center of extension along axis. Sonobuoy refraction data suggest that the basement consists of mixed igneous sedimentary material, atypical of mid-ocean ridges. On the basis of the near-surface manifestations of active faulting and magmatism, seafloor spreading will likely first occur in the Lower Delfín Basin. We suggest the transition to seafloor spreading is delayed by the lack of strain-partitioned and focused deformation as a consequence of shear in a broad zone beneath a thick sediment cover. *INDEX TERMS:* 0930 Exploration Geophysics: Oceanic structures; 0935 Exploration Geophysics: Seismic methods (3025); 3025 Marine Geology and Geophysics: Marine seismics (0935); 3040 Marine Geology and Geophysics: Plate tectonics (8150, 8155, 8157, 8158); 8109 Tectonophysics: Continental tectonics—extensional (0905); *KEYWORDS:* northern Gulf of California, oblique rifting, reflection seismic data, distributed deformation, sonobuoy refraction data

Citation: Persaud, P., J. M. Stock, M. S. Steckler, A. Martín-Barajas, J. B. Diebold, A. González-Fernández, and G. S. Mountain, Active deformation and shallow structure of the Wagner, Consag, and Delfín Basins, northern Gulf of California, Mexico, *J. Geophys. Res.*, *108*(B7), 2355, doi:10.1029/2002JB001937, 2003.

1. Introduction

[2] Our current understanding of the process of continental rifting and break up comes from three main sources. The first source is geophysical and geological observations in passive margins, intracontinental rift systems, and mature rifts; examples of these are the Galicia margin [*Boillot et al.*, 1989; *Manatschal and Bernoulli*, 1999], Australia margin [*Driscoll and Karner*, 1998], Okinawa Trough [*Herman et al.*, 1979], Bransfield Strait [*Barker*, 1998], Andaman Sea [*Curray et al.*, 1979], interior Sudan rifts [*McHargue et al.*, 1992] and Gulf of Suez [*Steckler et al.*, 1988]. Second, evidence on the rifting process is available from studies in areas that are actively undergoing continental break up, such as the Woodlark Basin, Papua New Guinea [e.g., *Taylor et al.*, 1995, 1999]; Red Sea [e.g., *Cochran and Martinez* 1988]; Asal Rift in the Gulf of Aden [e.g., *Manighetti et al.* 1998]; central Gulf of California, Mexico [e.g., *Saunders et al.*, 1982; *Einsele*, 1986], and Salton Trough, California [e.g., *Fuis and Kohler*, 1984; *Lonsdale*, 1989]. A third source of information is numerical and analog experimentation [e.g., *Clifton et al.*, 2000; *Lavier et al.*, 2000]. Observations in passive margins, intracontinental rift zones and mature rifts provide useful insight into prebreakup and postbreakup kinematics and the timing, extent and style of rifting, but they provide limited information on the processes active during breakup. Areas that are actively extending and thinning, enough to generate new crustal area, are few and poorly understood. In principle, numerical and analog experiments can provide information about the forces and different deformation paths of extending areas. However, in many cases the results are only valid for small strains, and experiments either cannot deal with the complex rheology

[1]Seismological Laboratory, California Institute of Technology, Pasadena, California, USA.
[2]Lamont-Doherty Earth Observatory, Columbia University, Palisades, New York, USA.
[3]Centro de Investigación Científica y Educaciõn Superior de Ensenada, Ensenada, Baja California, Mexico.

0148-0227/03/2002JB001937$09.00

of earth materials, or they introduce nonrealistic boundary conditions.

[3] The Pacific-North American plate boundary in the northern Gulf of California is an area of active continental breakup. Unlike the mouth of the Gulf where seafloor spreading began at ~3.5 Ma [*Bischoff and Henyey*, 1974; *DeMets*, 1995; *Lonsdale*, 1989], the northern Gulf still lacks seafloor spreading, despite at least 255 ± 10 km of separation between the rifted margins that would have required formation of considerable new crustal area [*Oskin et al.*, 2001]. The oceanic plate boundary of the southern and central Gulf comprises narrower zones of deformation, e.g., the Guaymas Basin and Ballenas Transform fault zone (Figure 1a). The northern Gulf, in contrast, contains a broader zone of diffuse deformation akin to the continental domain of southern California. It is expected that a plate boundary should narrow as it passes from a continental regime, such as southern California, to an oceanic regime, such as the southern Gulf of California [*Molnar*, 1988]. Along a transcurrent boundary, this localization process may differ because of differences in the rheology of the lithosphere, the heat flow, tectonic style and the amount and type of new crust being produced. On the basis of the high sedimentation rates and lack of evidence of seafloor spreading, the northern Gulf crust is expected to be similar to the transitional crust identified in drill samples in the central Gulf of California [*Saunders et al.*, 1982] and interpreted from seismic velocities in the Salton Trough [*Nicolas*, 1985]. This active transcurrent plate boundary, thus, presents an excellent opportunity for studying the influence of obliquity and transitional crust on the style of deformation and the progression from continental breakup to seafloor spreading.

[4] In this paper, we identify the northern Gulf of California as the region of the Gulf north of latitude 28.5° (Figure 1). The major transform faults and extensional basins of the northern Gulf of California include, from north to south, the Cerro Prieto fault (southernmost fault of the San Andreas fault system), the Wagner Basin, the Delfín Basins and the Ballenas Transform fault system (Figure 1b). These active segments of the plate boundary have been identified from seismicity and seafloor morphology. Details of the tectonic and sedimentary history of the northern Gulf of California have, however, been obscured by high sedimentation rates and a low rate of large earthquakes.

[5] The most detailed interpretation of the tectonics of the northern Gulf to date is based on single channel seismic reflection data acquired in 1970 [*Henyey and Bischoff*, 1973]. From these data, *Henyey and Bischoff* [1973] developed a fault map of the northern Gulf; their interpretations of the seismic data were, however, limited by interbed multiples and reverberations derived from the source signal. Several deeper multichannel seismic (MCS) reflection profiles were collected during the 1996 cruise of the Spanish ship *Hespérides* in the Gulf of California. Within our survey area, one seismic line ran across the Delfín Basin (Figure 1b) [*González-Fernández et al.*, 1999] showing distributed faulting with many active and inactive faults. Another seismic profile across the Lower Delfín Basin and Ballenas-Salsipuedes channel (Figure 1b) found evidence for intense magmatism in the Salsipuedes Basin which decreased northward into the Lower Delfín Basin [*Paz-López*, 2000]. A representative industry seismic line across the northern Gulf, showing steeply dipping, sinuous faults that cut the entire sedimentary column, was also published by *Pérez-Cruz* [1980], but this line did not image the near surface strata with high resolution, nor result in an integrated fault map showing the active kinematics of the region. Thus many questions about the modern fault system remain.

[6] We have collected a grid of high-resolution MCS reflection data and sonobuoy refraction data in the northern Gulf of California. The quality of these data along with the wide spatial coverage and high-precision navigation allow us to provide an improved fault map, defining in detail the style of faulting in the area surveyed. Our study also constrains the depth to basement near the Baja California coast and maps recent volcanic features on the seafloor.

2. Geologic and Tectonic Background

[7] Extension in the Gulf of California appears to have started after 12 Ma along a ~24−12 Ma subduction-related volcanic arc [*Gastil et al.*, 1979; *Sawlan*, 1991]. A mid to late Miocene period of possibly minor extension [*Karig and Jensky*, 1972; *Stock and Hodges*, 1989] occurred at the site of the future Gulf with transform motion west of the future Baja Peninsula. At this time, a broad area east of the future Gulf, from southern Arizona and New Mexico to the Gulf Extensional Province was undergoing extension [*Henry and Aranda-Gómez*, 2000; *Humphreys and Weldon*, 1991]. At approximately 6 Ma, the plate boundary jumped inland to the Gulf of California [*Lonsdale*, 1989; *Oskin et al.*, 2001] and marine sediments were widely deposited in the northern Gulf [*Helenes and Carreño*, 1999]. The plate margin subsequently evolved into a series of long transform faults connected by smaller

Figure 1. (opposite) (a) Map of the Gulf of California. Heavy box outlines the survey area, which is shown in more detail in Figure 1b. Black arrows indicate the current Pacific-North America relative plate motion direction, N37°W [*Atwater and Stock*, 1998]. Pacific-North America plate boundary faults and spreading centers are from *Fenby and Gastil* [1991]. The major rift basins in the Gulf are labeled. (b) Location of multichannel seismic lines in the northern Gulf of California collected by the *Ulloa* in 1999. Stars mark sonobuoy locations. Seismic profiles shown in this work are marked with thick black lines and labeled. Arrowheads mark the right ends of the plotted seismic data. Lines 6 and 17 are shown in figures only. The rest of the seismic profiles are shown in foldouts, which refer to figures for more detail. ABF, Agua Blanca Fault; BTF, Ballenas Transform Fault Zone; CPF, Cerro Prieto Fault; CR, Consag Rock; EF, Elsinore Fault; EPR, East Pacific Rise; GB, Gonzaga Bay; IA, Isla Angel de la Guarda; IF = Imperial Fault; ISL = Isla San Luis; SAFZ, San Andreas Fault Zone; SJF, San Jacinto Fault; SB, Salsipuedes Basin; SMF, San Miguel Fault; SPMF, San Pedro Mártir Fault; ST, Salton Trough; TB, Tiburón Basin; TI, Tiburón Island; VP, Volcán Prieto. W1, W2, and W3 are PEMEX proprietary wells. See color version of this figure at back of this issue.

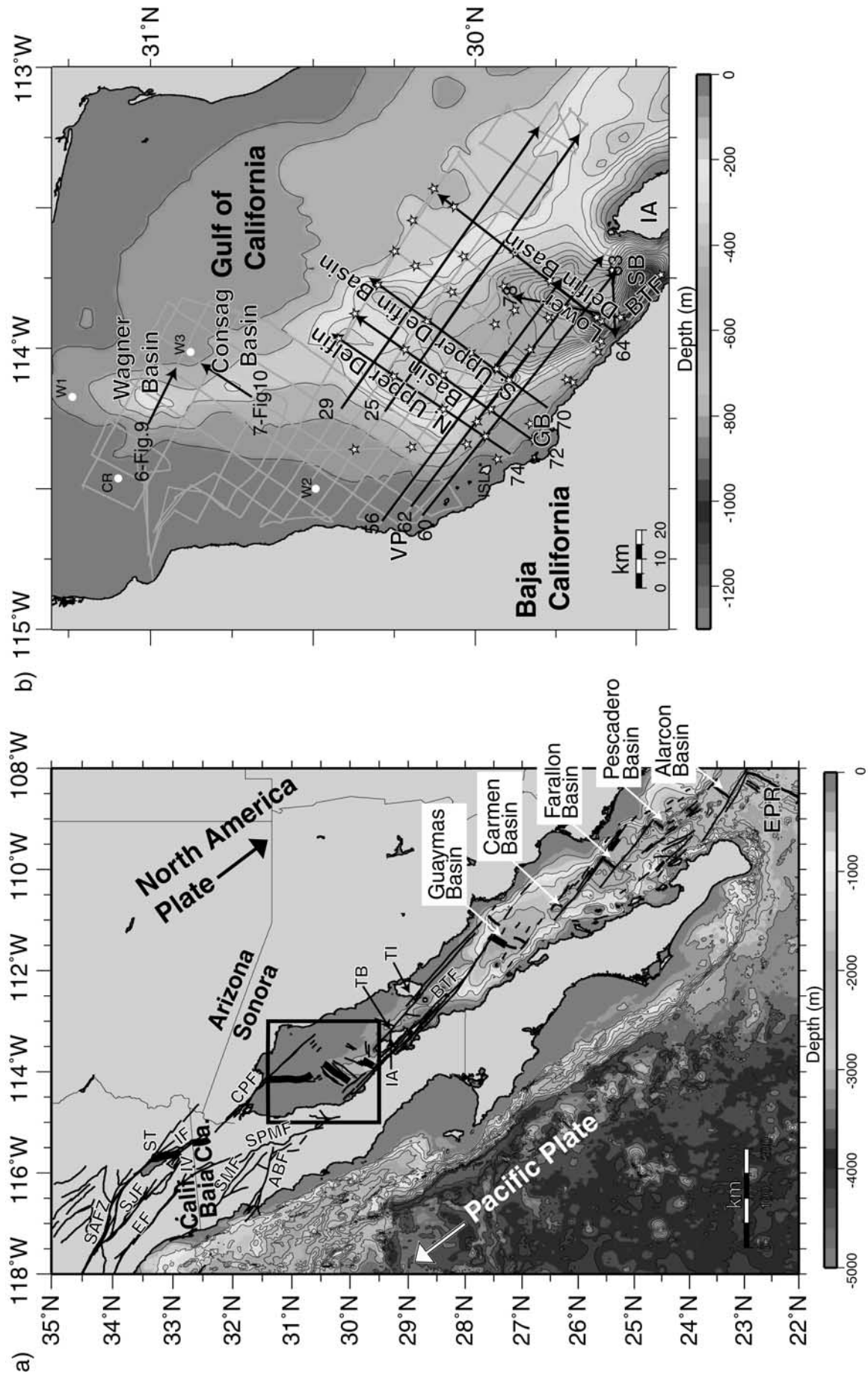
a)
b)
North America Plate
Pacific Plate
Arizona
Sonora
Baja Ca.
Calif.
Gulf of California
Baja California
Wagner Basin
Consag Basin
N. Upper Delfin Basin
S. Upper Delfin Basin
Lower Delfin Basin
Guaymas Basin
Carmen Basin
Farallon Basin
Pescadero Basin
Alarcon Basin
EPR
SAFZ
SJF
EF
IV
IF
ST
SMF
SPMF
ABF
CPF
TB
TI
BTF
IA
SB
GB
ISLD
VP
CR
W1
W2
W3
6-Fig.9
7-Fig10
29
25
56
62
60
74
72
70
78
64
83
km
Depth (m)

rift basins. Seafloor spreading type magnetic anomalies are, however, only observed in the Alarcón Basin and southward (Figure 1a) [*Klitgord et al.*, 1974; *Larson*, 1972; *Lawver et al.*, 1973; *Sánchez-Zamora et al.*, 1991; *Ness et al.*, 1991].

[8] The centers of extension in the northern Gulf have jumped westward in several cases, and thus lie toward the western side of the rift. Around 3.3 Ma the locus of extension in the northern Gulf jumped westward from Tiburón Basin to the Upper Delfín Basin, with the Wagner and southern Tiburón Basins still active parts of the plate boundary [*Lonsdale*, 1989; *Stock*, 2000] (Figure 1a). The current structures in the northern Gulf originated after yet another westward relocation of the plate boundary sometime after 2 Ma, as spreading jumped from the southern Tiburón Basin to the Lower Delfín Basin and the Ballenas transform fault became the major transform fault in this region [*Lonsdale*, 1989; *Stock*, 2000] (Figure 1). The Wagner Basin is also closer to the western side of the rift and may have jumped from a previous location to the east or SE [*Aragón-Arreola et al.*, 2002].

[9] The Ballenas transform fault system has well-defined en echelon transform zones subparallel to relative plate motion. There is, however, a 10° change in strike between the Ballenas transform fault and the Cerro Prieto fault to the north [*Goff et al.*, 1987] (Figure 1a). Geological data and earthquake patterns suggest that some of the slip is transferred from the northern end of the Ballenas Transform fault to the transpeninsular faults located in the continental crust of Baja California [e.g., *Goff et al.*, 1987] (Figure 1a). It is estimated that between 7 and 15 mm/yr of right-lateral slip is accommodated by these faults [*Bennett et al.*, 1996; *Humphreys and Weldon*, 1991; *Goff et al.*, 1987]. There is, however, no clear evidence that the faults are physically linked [*Stock and Hodges*, 1989, 1990] or interact through their stress fields [*Frez and González*, 1991]. Seismological observations rather suggest distributed deformation [*Frez and González*, 1991; *Thatcher and Brune*, 1971]. The exact way in which slip is transferred into the Gulf of California is not known.

[10] From the Salton Trough southward, the crust thins from a minimum thickness of 21 km to 13 km and 10 km in the northern and central Gulf respectively, where the thinnest crust is found along the peninsular coast [*Couch et al.*, 1991]. In the southern Gulf, the crust is 8 km thick and crustal thinning is symmetrical [*Couch et al.*, 1991]. Seismic refraction studies in the northern Gulf require a crustal thickness of ~20–25 km and a crustal structure that is similar to that found in the continental borderland of Southern California [*Phillips*, 1964]. More recent work also constrains crustal thickness for the northern Gulf and indicates that its seismic properties are not typical of oceanic crust. Along a profile at ~31°N latitude, Moho depth estimates from *P*-to-*S* converted phases increase from ~33 ± 3 km near the Pacific coast of Baja California to ~40 ± 4 km beneath the western part of the Peninsular Ranges batholith [*Lewis et al.*, 2001]. The crustal thickness then decreases rapidly across the eastern Peninsular Ranges and Main Gulf Escarpment to a fairly uniform thickness of ~15–18 ± 2 km within and on the margins of the northern Gulf [*Lewis et al.*, 2001]. This eastward thinning

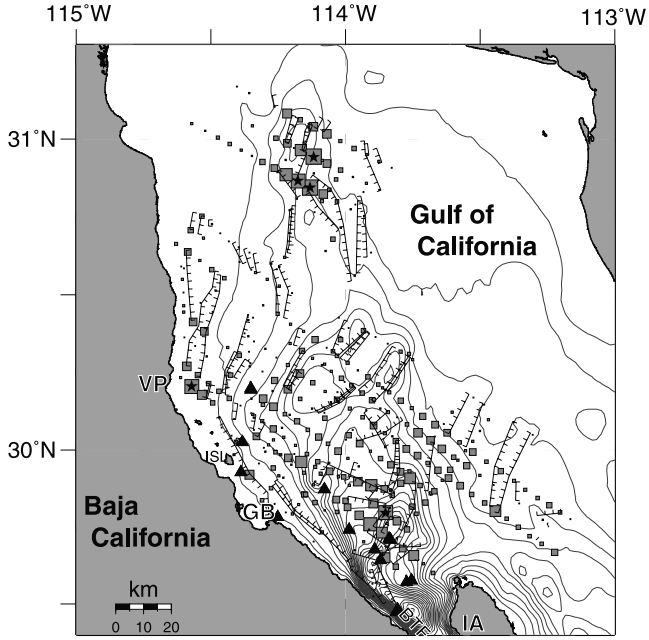

Figure 2. Map of faults that were interpreted on more than one seismic profile (black lines). Hachures mark the downthrown sides of faults. Gray lines are bathymetric contours every 50 m. Gray boxes indicate the fault density of all the picked faults (number of faults per 5 km along track). The largest and smallest boxes contain 20 faults and 1 fault respectively and the surveyed area has a mean fault density of approximately three faults per 5 km. Stars mark areas with 18 or more faults per 5 km. Solid triangles mark the locations of volcanic knolls identified in the seismic profiles. See Figure 1b for place abbreviations.

of the crust may have resulted from diffuse lower crustal extension beneath the Salton Trough and northern Gulf [*Lewis et al.*, 2001]. In addition, from the analysis of deep seismic profiles and new gravity data, *González-Fernández et al.* [1999] place the bottom of the crust at ≥16–17 km in the Upper Delfín Basin and ≥18–19 km beneath Tiburón Basin, to the southeast of our field area (Figure 1a). A structural high is interpreted between these two basins, where the crust is 21 km thick [*González-Fernández et al.*, 1999; A. González-Fernández, manuscript in preparation, 2003].

[11] A significant part of this crust is sedimentary. On the basis of stratigraphic analysis of two Petróleos Mexicanos (PEMEX) wells, the up to 2 km thick sedimentary package imaged during our survey may be no older than Pleistocene in age, perhaps with some Pliocene strata at the base. The PEMEX well W2 (Figure 1b) shows basement consisting of a quartz-bearing diorite at a depth of 2950–3191 m (PEMEX, unpublished data, 1981–1982). An igneous unit of altered andesite (~150 m thick) overlies the basement and has a whole rock K/Ar age of 8 ± 1 Ma. The entire sedimentary sequence above this igneous unit is Quaternary-Pleistocene in age. Indeed, *Van Andel* [1964] estimates a sedimentation rate in the northern Gulf of 3.16 km/m.y. From bottom to top, the sedimentary unit consists mainly of consolidated, semiconsolidated and poorly consolidated sandy mudstones. Marine beds in the top kilometer of

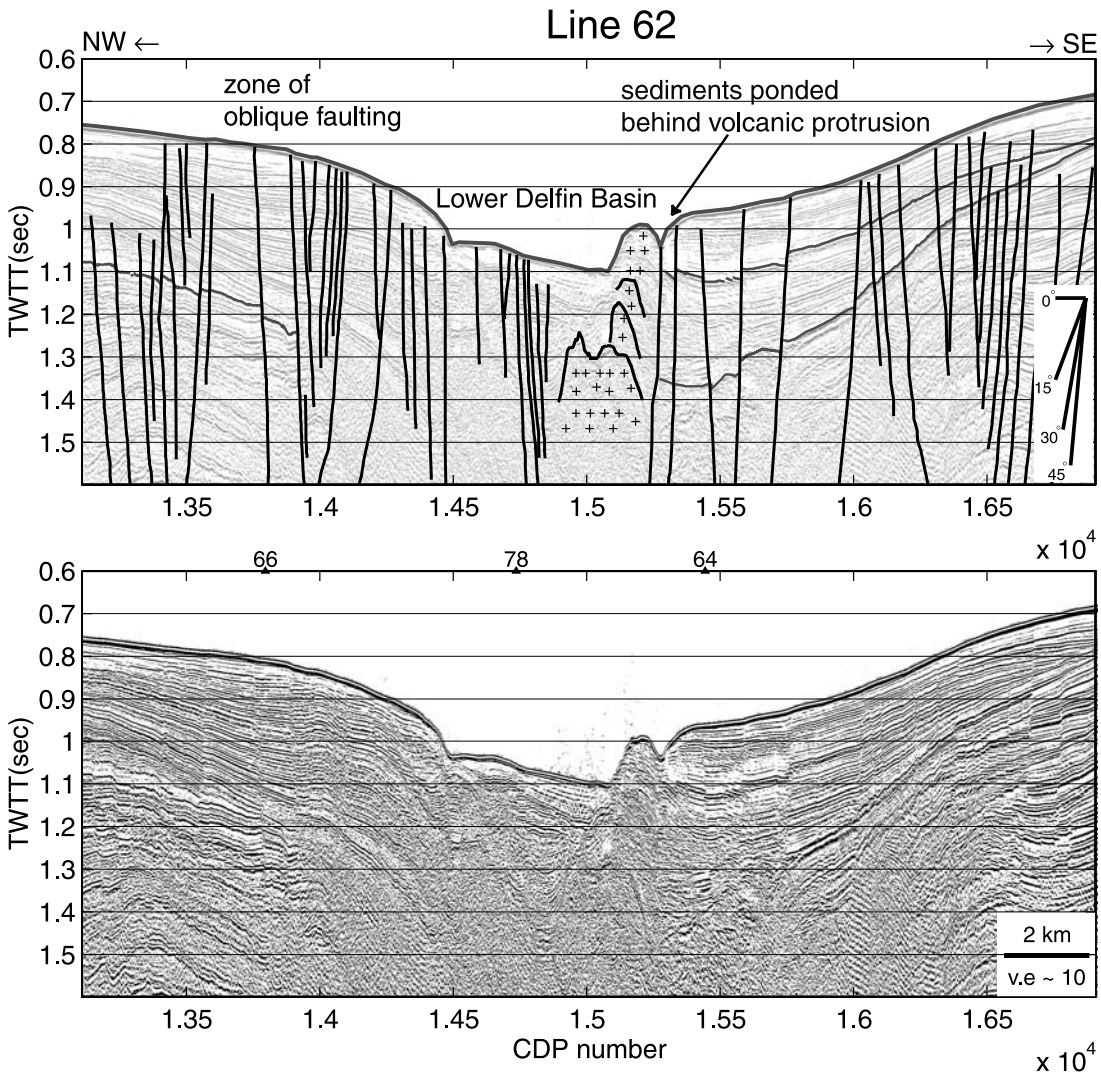

Figure 3. Profile perpendicular to the axis of the Lower Delfín Basin and SE of the profile shown in Figure 5. Isla Angel de la Guarda lies a few kilometers SE of this profile. The most prominent reflectors are highlighted. These reflectors were not traceable across the axial region of the southwestern end of the LDB (shown here), where layers are disrupted by the intrusion of magma.

sediments contain abundant mollusk bioclasts. The PEMEX well W3 (Figure 1b) penetrated Recent-Pleistocene sediments down to 2540 m; from 2560 to 3000 m the ages are undetermined.

3. Data and Analysis

[12] We used Lamont-Doherty Earth Observatory's high-resolution multichannel seismic (MCS) system with differential GPS navigation to obtain a 2-D grid of 3500 km of reflection data in May–June 1999 aboard Centro de Investigación Científica y Educaciōn Superior de Ensenada's (CICESE) 28 m research vessel B/O *Francisco de Ulloa* (Figure 1b). The reflection equipment imaged to subbottom depths of up to 2 km. 48 expendable sonobuoys were also deployed during the cruise (Figure 1b); 43 of these returned usable records and provide velocities to greater depth. 4000 km of 12.5 and 208 kHz echo sounder data were also collected. In addition, well data from PEMEX are now available to the CICESE research group and are here used to constrain the depth to basement and stratigraphy in the northern Gulf.

[13] The seismic reflection data were acquired with a 48 channel, 600 m streamer, at a sampling interval of 1 ms (shot spacing of 12.5 or 25 m) and were recorded for 2–3 s. A Generator-Injector air gun provided a cleaner source pulse than the Bolt air gun used by *Henyey and Bischoff* [1973]. The processing sequence of the reflection data is as follows: (1) timing corrections, (2) trace edit, (3) velocity analysis based on semblance coefficients, (4) normal moveout and stack, (5) spherical divergence correction, (6) predictive deconvolution (with filter length of 30 ms and gap of 16 ms), (7) Stolt migration, (8) band-pass filter (30–240 Hz), and (9) time-variant gain. (The entire data set is available through the MapApp tool, which is downloadable at http://ocean-ridge.ldeo.columbia.edu/MapApp/MapAppJava.html.) We interpreted the data using the general techniques outlined by *Badley* [1985] and the criteria for identifying strike-slip zones given by *Harding* [1990]. Strikes of the major faults (black lines in Figure 2) were

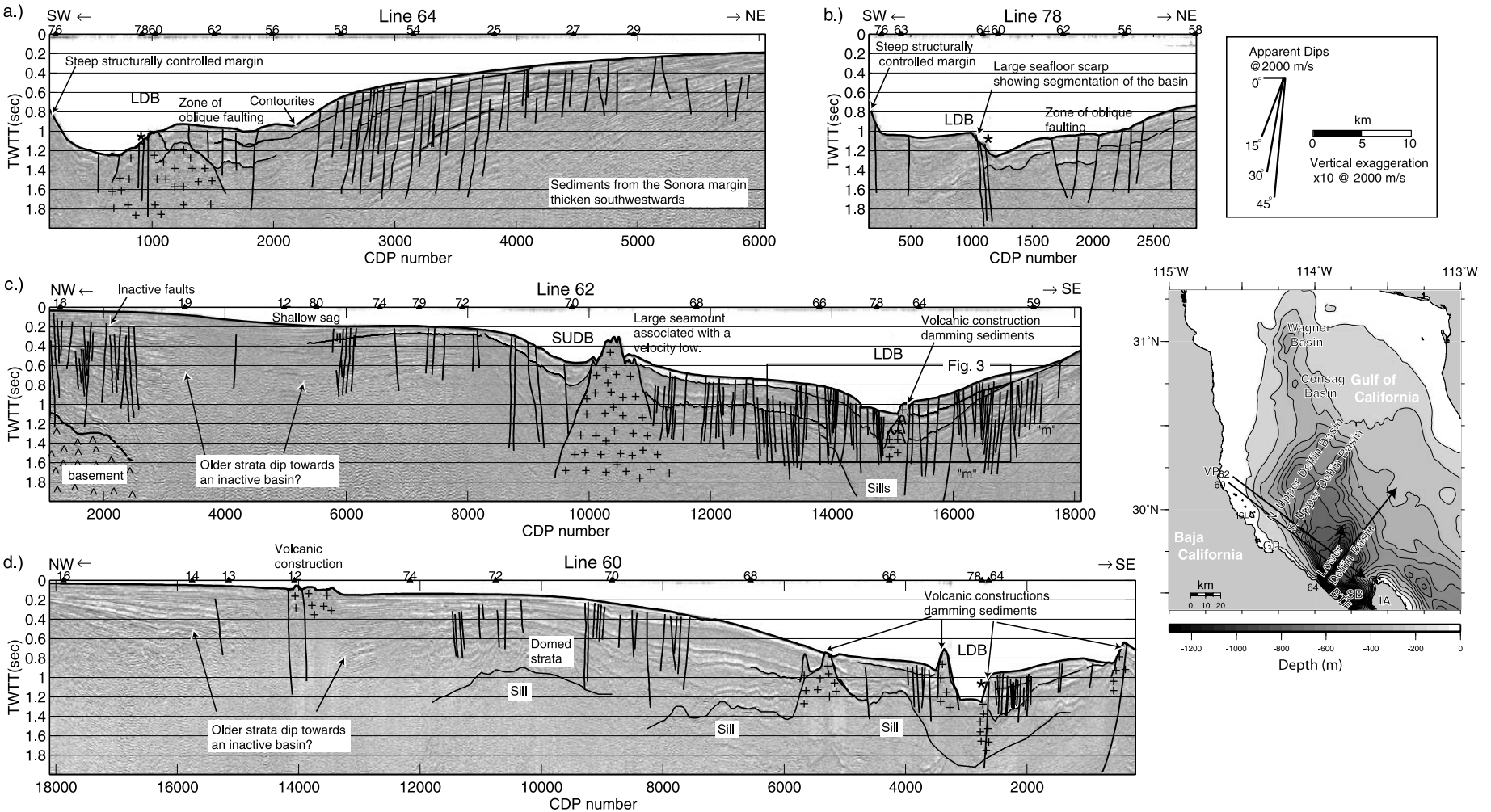
a.)
SW ←
Line 64
→ NE
Steep structurally controlled margin
LDB
Zone of oblique faulting
Contourites
Sediments from the Sonora margin thicken southwestwards
TWTT(sec)
CDP number
b.)
SW ←
Line 78
→ NE
Steep structurally controlled margin
Large seafloor scarp showing segmentation of the basin
LDB
Zone of oblique faulting
Apparent Dips @2000 m/s
km
Vertical exaggeration x10 @ 2000 m/s
c.)
NW ←
Inactive faults
Line 62
→ SE
Shallow sag
SUDB
Large seamount associated with a velocity low.
Volcanic construction damming sediments
LDB
Fig. 3
basement
Older strata dip towards an inactive basin?
Sills
"m"
d.)
NW ←
Volcanic construction
Line 60
→ SE
Volcanic constructions damming sediments
Domed strata
Sill
LDB
Older strata dip towards an inactive basin?
115°W
114°W
113°W
31°N
30°N
Wagner Basin
Consag Basin
Gulf of California
Upper Delfin Basin
Lower Delfin Basin
Baja California
GB
SB
IA
VP
km
Depth (m)

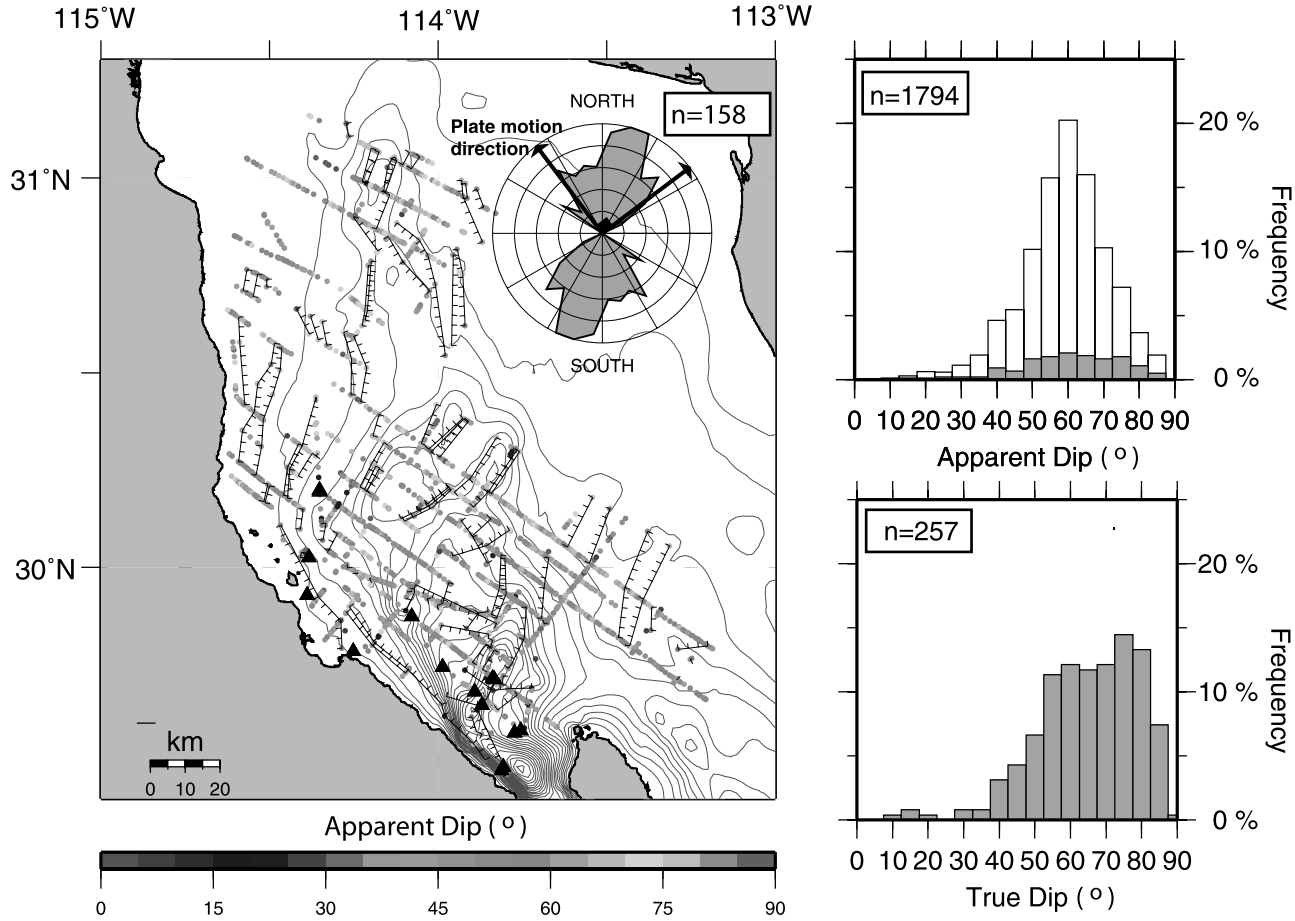

Figure 4. Map showing the apparent dips of all interpreted faults (total of 1794), calculated in the plane of the seismic profiles with a mean seismic velocity of 2000 m/s. Gray lines are bathymetric contours every 50 m. Strikes of all faults that were imaged on at least two seismic profiles (black lines) are shown in the inset rose diagram. This rose plot is normalized for equal area and shows a total of 158 fault segments or 112 faults with the maximum radius representing 24 fault segments. Note the approximate trends of the major rift basins are LDB = N10°E, NUDB and SUDB = N35°E and WB = N25°E (Figure 11). The dominant strike of faults in the survey area is N-N30°E, which is within 5–10° of the trend of the major rift basins. The top histogram shows the apparent dips of all faults; the gray shaded area represents the apparent dips of the faults shown by black lines in the map. The bottom histogram shows the true dip of these faults, which were calculated using the strikes. See color version of this figure at back of this issue.

determined. We used these strikes along with the apparent dips to calculate true dips of the major faults.

[14] The sonobuoy or refraction data were first decimated and filtered. Seafloor reflection and direct arrivals were modeled to determine the source-receiver offsets. An offset-based linear time reduction was used to bring the interpretable arrivals within a convenient window for analysis. Interactive ray tracing was used to create velocity models.

4. Multitude and Density of Faulting

[15] One of our most striking observations in the northern Gulf of California is the large number of faults and the

Foldout 1. (opposite) Compilation of MCS profiles (a) 64, (b) 78, (c) 62, and (d) 60, which cross the Lower Delfín Basin. Locations of the seismic profiles are shown in the map and Figure 1b. Arrowheads mark the right end of the images. Box in Foldout 1b marks the location of Figure 3. The *y* axis is two-way travel time (TWTT), and the *x* axis is common depth point number (CDP number). Vertical exaggeration is ~10 for all panels. The numbered black triangles along the top of the plots represent crossing lines. A dredge sample from the volcanic knoll in the southeastern flank of the SUDB (Foldout 1c) was found to be rhyolite pumice [*Henyey and Bischoff*, 1973]. The large normal fault around CDP 10000 in Foldout 1c strikes northeastward into the SUDB. Volcanic rocks shown in Foldout 1a form a ridge across the axis of the Lower Delfín Basin, separating the NE trending basin into two subbasins. The subbasin to the SW reaches the NW end of the Ballenas Transform Fault zone and is faulted obliquely. Oblique faults also cut across the axis of the basin in the area of the contourites (Foldout 1a). Pluses indicate volcanic constructions, and wedges indicate well-resolved acoustic basement; "m", seafloor multiple.

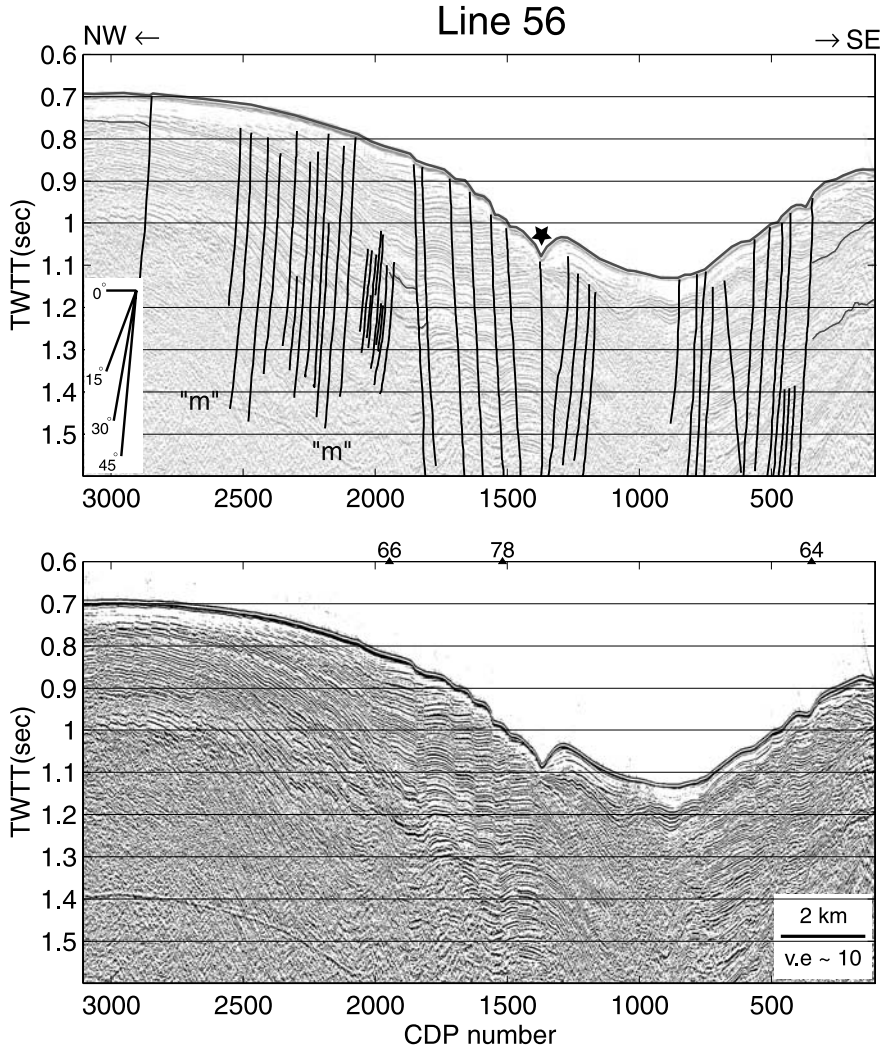

Figure 5. Profile perpendicular to the axis of the Lower Delfín Basin. Note the opposing dips of the faults in the northwestern flank of the basin. The large seafloor scarp around CDP 1300 (marked by the star) could be an indication of strike-slip offset. Overlapping E-W striking faults with oblique offset crosscut the Lower Delfín Basin (see Figure 2), which may be a pull-apart basin.

broad area over which faulting occurs (Figure 2). Here, we describe the style of faulting with respect to the major rift basins and possible transform fault zones, i.e., the Ballenas Transform Fault (BTF). The northern Gulf of California is composed of three sets of active basins distributed within a broad shallow depression: (1) the Lower Delfín Basin (LDB) and Salsipuedes Basins, (2) the Northern Upper Delfín Basin (NUDB) and Southern Upper Delfín Basin (SUDB), and (3) the Wagner Basin (WB) and Consag Basin (CB) (Figure 1b). We have grouped together basins in sets 1 and 2 based on their proximity and structural similarities/connections. The WB and CB may not be structurally similar but are grouped together based on their similar orientation and shallow relief.

4.1. Lower Delfín and Salsipuedes Basins

[16] Along trend, the northern half of the LDB has a higher fault density than the southern half, with ~18 faults in 5 km in the northwest flank (stars in Figure 2). The high density of faulting is also shown in the seismic profile in Figure 3 where many small fault blocks are rotated and tilted basinward. Although strata in both flanks of the LDB are highly faulted, fault offsets are small, tens of meters or a few meters (at a mean seismic velocity of

Foldout 2. (opposite) Compilation of MCS profiles (a) 74, (b) 72, (c) 70, and (d) 63, which cross the NW extension of the Ballenas Transform Fault Zone. The dashed line in Foldouts 2a, 2b, and 2c represents the master fault in the northward extension of the BTF. Locations of the seismic profiles are shown in the map and Figure 1b. Arrowheads mark the right end of the images. See Foldout 1 caption for further details.

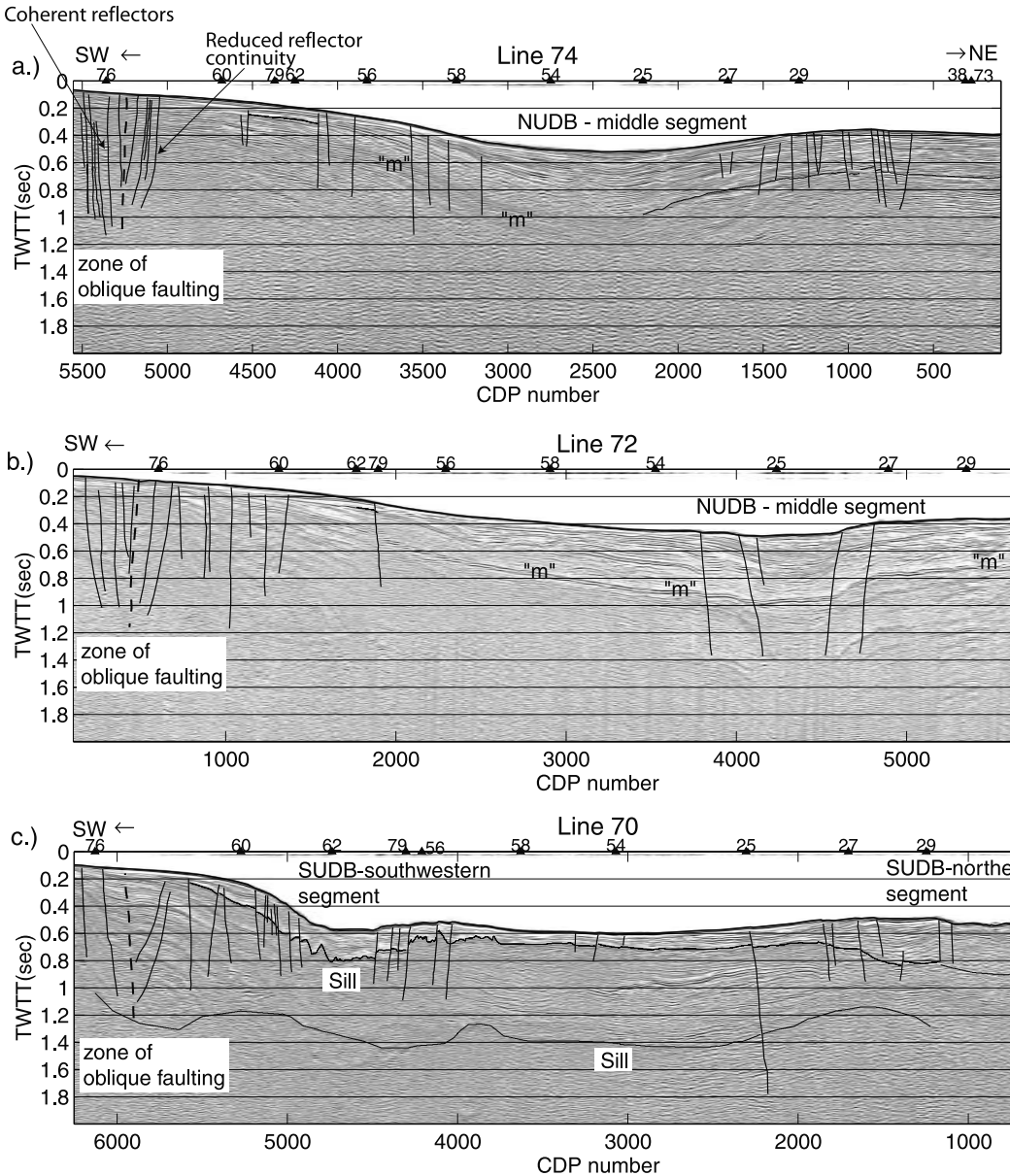
a.)
Coherent reflectors
Reduced reflector continuity
SW ←
Line 74
→NE
NUDB - middle segment
"m"
zone of oblique faulting
TWTT(sec)
CDP number
b.)
SW ←
Line 72
→ NE
NUDB - middle segment
zone of oblique faulting
TWTT(sec)
CDP number
c.)
SW ←
Line 70
→NE
SUDB-southwestern segment
SUDB-northeastern segment
Volcanics at the seafloor
Sill
zone of oblique faulting
TWTT(sec)
CDP number

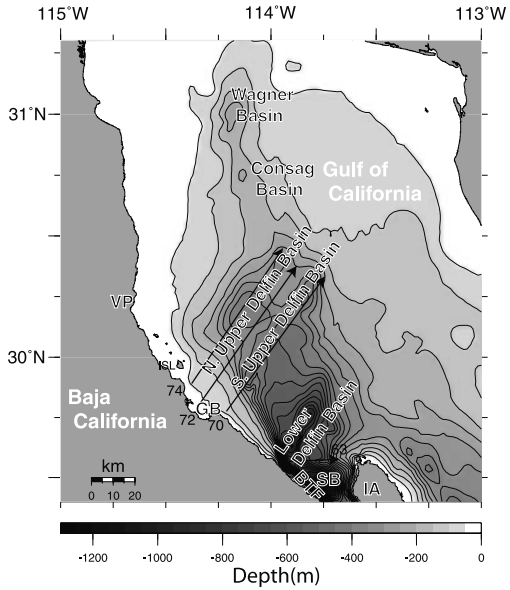
115°W
114°W
113°W
31°N
30°N
Wagner Basin
Consag Basin
Gulf of California
Baja California
VP
N. Upper Delfin Basin
S. Upper Delfin Basin
Lower Delfin Basin
GB
SB
IA
km
Depth(m)
Apparent Dips @2000 m/s
Vertical exaggeration x10 @ 2000 m/s

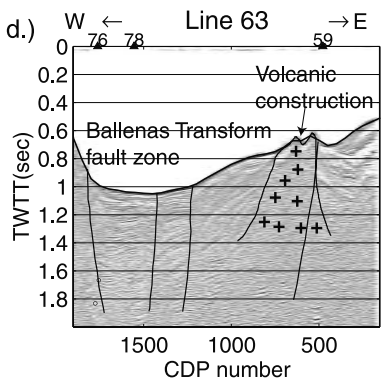
d.)
W ←
Line 63
→E
Volcanic construction
Ballenas Transform fault zone
TWTT(sec)
CDP number

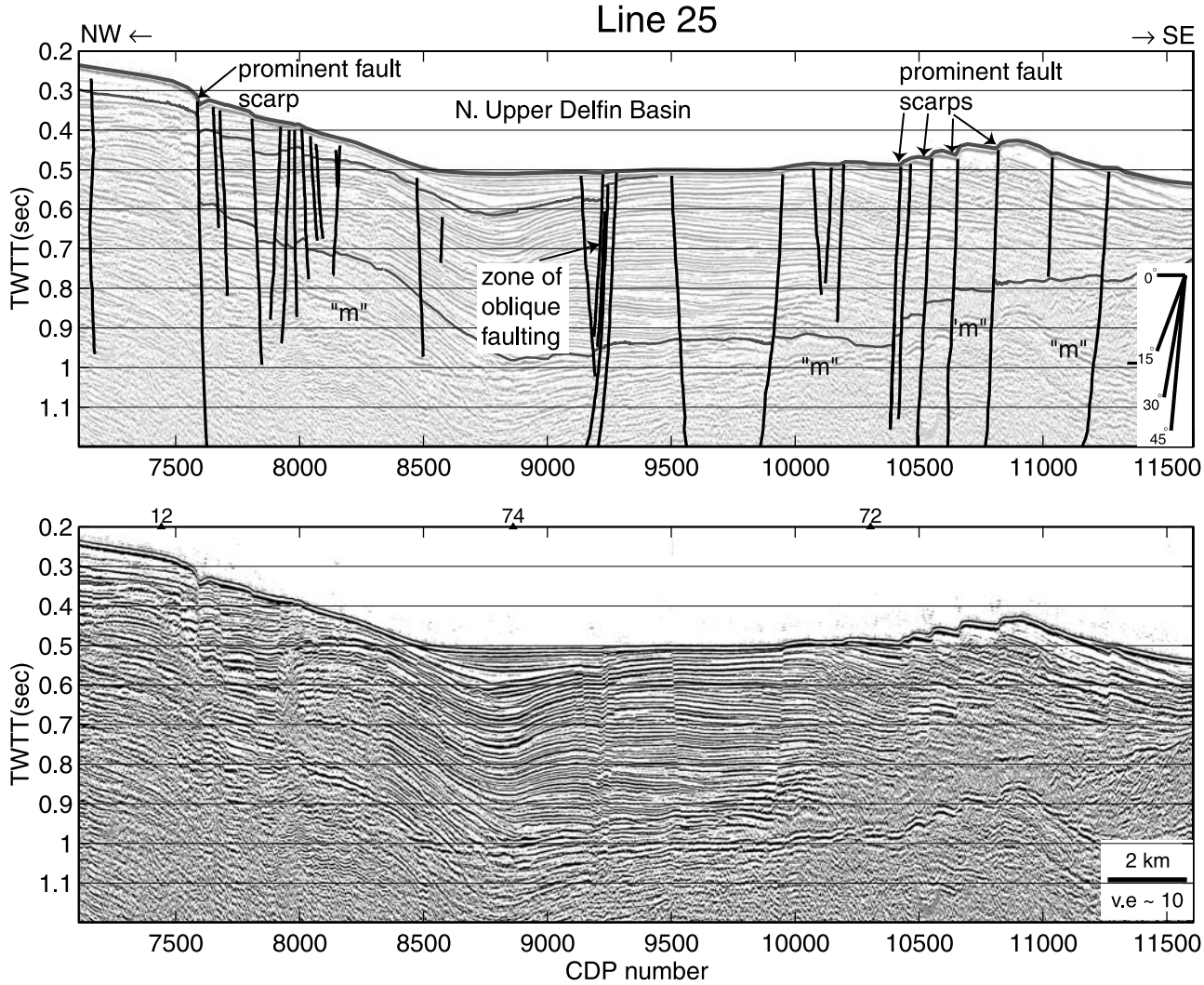

Figure 6. Seismic profile across the axis of the NUDB. Here the middle segment of the NUDB is more active than the middle segment of the SUDB in Figure 7. Note the multiple faults and the large seafloor scarps (~25 m at water velocity of 1500 m/s).

2000 m/s) compared to the main normal faults that bound the basin, which have offsets of 100 m or more based on seafloor scarps (Foldouts 1a and 1b, lines 64 and 78). Inactive faults are uncommon in the survey area, but some were imaged 10–15 km away from the basin's axis (Foldout 1c, line 62). Although fault dips vary significantly, most faults in the flanks of the LDB have apparent dips of ~50–60° (Figure 4), with opposing dips common (Figure 5). In general, the dip direction of faults changes across the basin's axis, with mainly east dipping faults in the NW flank and west dipping faults in the SE flank (Figure 5).

4.2. Extension of the Ballenas Transform Fault?

[17] Northwest of Isla Angel de la Guarda, oblique faults strike into the LDB (Figure 2). To the southwest, the LDB is faulted obliquely, by faults extending from the Ballenas Transform Fault zone northward (Figure 2 and Foldout 2d), line 63). These faults merge into a diffuse zone of negative flower structures, which may mark the northwestern end of the BTF. Negative flower structures were identified in several seismic profiles close to the Baja California coast and just north of Isla Angel de la Guarda (to the SW in Foldouts 2a, 2b, and 2c, lines 74, 72, and 70). This discontinuous zone of oblique faulting along the Baja California coast (e.g., Foldout 2c, line 70 around CDP 6000) extends from the southwestern end of the LDB northwestward toward Isla San Luis (Figure 2). The fault splays are disrupted along this zone and mostly bound blocks that are downdropped in a normal sense. The sag in the negative flower structure is evident farther north where the master fault (Foldout 2a, ~CDP 5500, line 74) juxtaposes two distinctly different sedimentary packages. On the northeastern side of the master fault we see a series of incoherent reflectors with reduced reflector continuity, which may consist of sediments that have been baked by intrusions, or that contain gas or volcanic deposits. Across the master fault, this block is in contact with a well-layered sedimentary package indicating lateral offset. The master fault intersects basement below 1 s TWTT. The

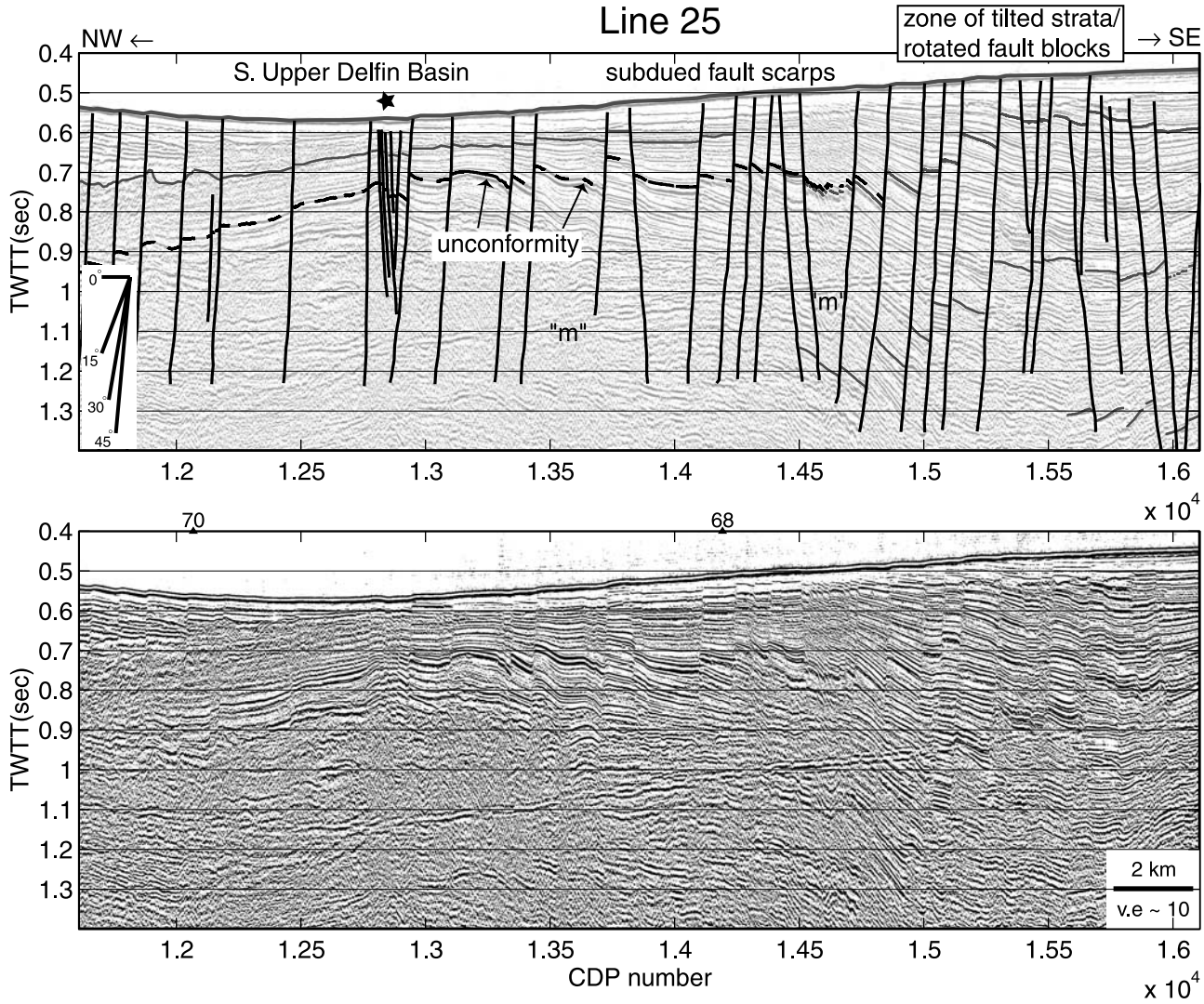

Figure 7. Seismic profile across the axis of the SUDB. The SUDB is subdued in this region, but is more active in its northeast and southwest segments. Strike-slip or oblique offset is suggested in the center of the image around CDP 13000 (marked by the star). Layers thicken both to the NW and SE of this zone of oblique offset. Prominent reflectors are highlighted in the top panel. The dashed line marks an unconformity.

shallow depths to basement in this area are confirmed by the sonobuoy velocities.

4.3. Northern and Southern Upper Delfín Basins

[18] These subparallel basins are divided into three segments along axis. This segmentation is expressed in the bathymetry (Figure 1b) and faulting. Although both basins are sites of active deformation, the center of extension switches along the axes from one basin to the next. Along seismic line 25, the seafloor scarps in the middle segment of the NUDB (Figure 6) are more pronounced and faults are more closely spaced than in the middle of the SUDB (Figure 7). Faulting in the northeast and southwest segments of these basins displays the opposite pattern, with smaller fault scarps in the NUDB than the SUDB (Foldouts 3a and 3c and Figure 8). In a profile across the northeast segment of the Upper Delfín Basins (Foldout 3c, line 29), the seafloor scarps in the NUDB are only a few meters, whereas the scarps farther south in this basin (Foldout 3b and Figure 6) measured a few tens of meters. To the southwest in this profile (Foldout 3c, line 29), the seafloor scarps in the SUDB are large (~CDP 14500). In the southwest segment of the SUDB, near the volcanic protrusion in Foldout 1c [*Henyey and Bischoff*, 1973], this basin is more active than the NUDB. As the middle segment of the SUDB is approached from the south (Figure 8), deformation lessens and the basin becomes shallower. This asymmetry in active faulting is, however, not evident in the fault density map (Figure 4), where both basins appear equally active.

[19] Compared to faults in the SUDB, those in the NUDB are steeper (Figure 4) and reversals in the dip direction of faults are more common. As in the LDB, the same overall pattern of east dipping faults in the NW flank of the rift basin and west dipping faults in the SE flank is observed in the NUDB and northeast and southwest segments of the SUDB;

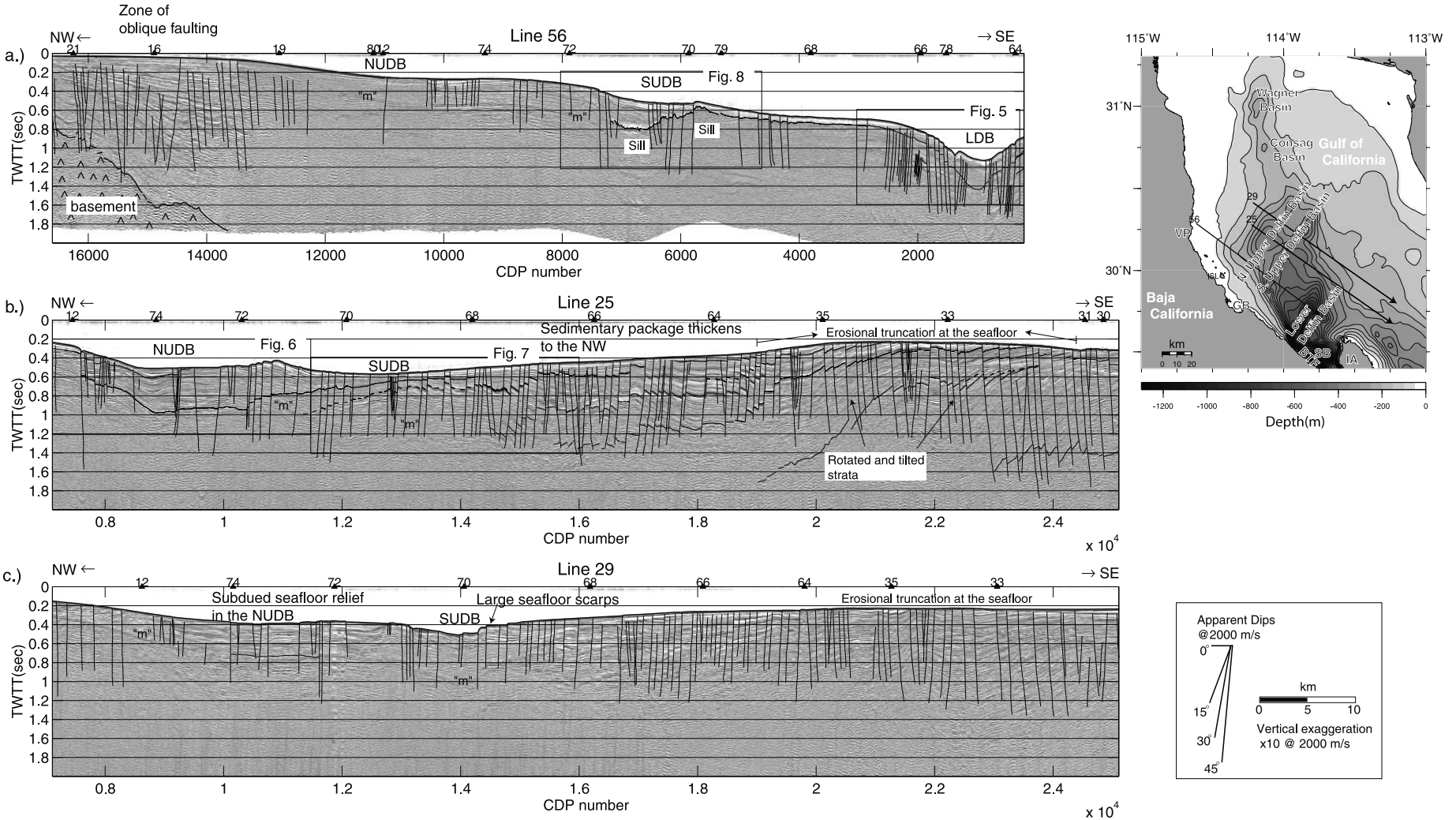

Foldout 3. Compilation of MCS profiles (a) 56, (b) 25, and (c) 29, which cross the Upper Delfín Basins. Locations of the seismic profiles are shown in the map and Figure 1b. Arrowheads mark the right end of the images. Boxes mark the location of other illustrations. See the caption in Foldout 1 for further details.

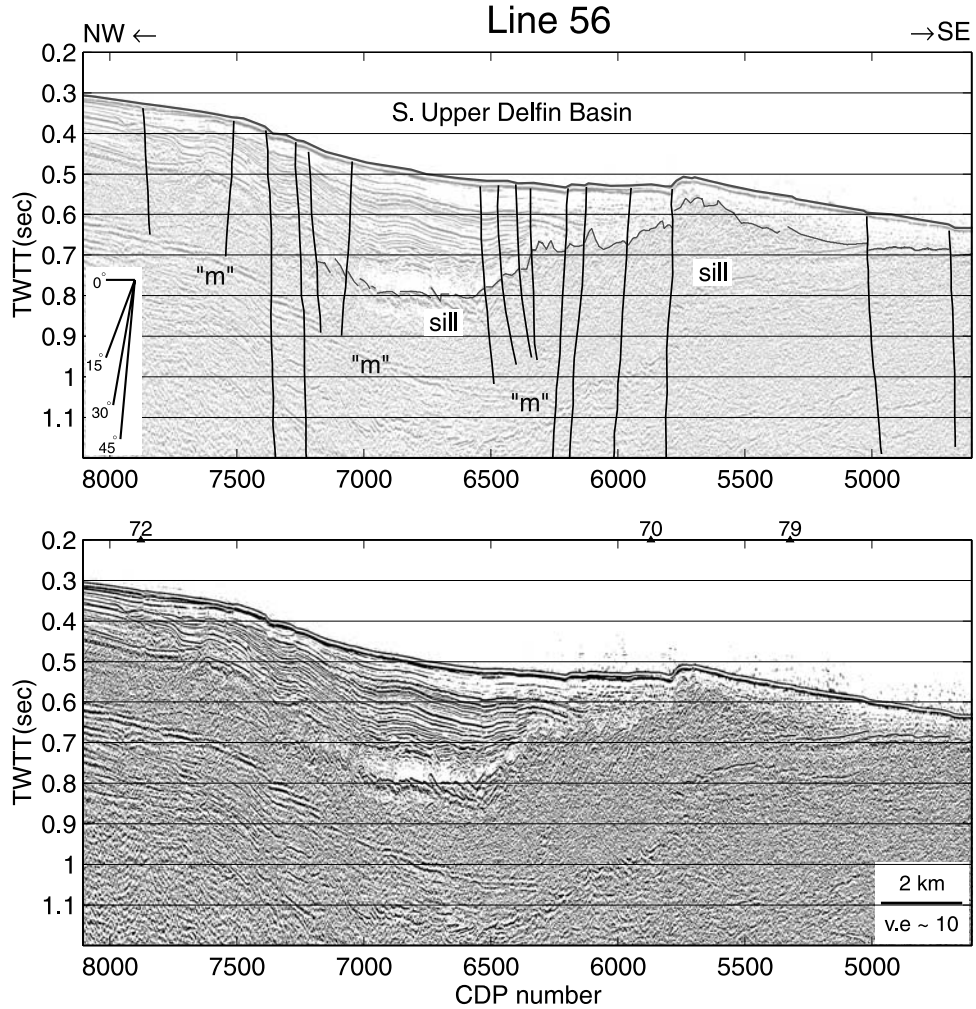

Figure 8. Seismic profile across the axis of the SUDB. Note that the seafloor relief of the SUDB is subdued and the fault scarps are not very large. This profile shows that extension is decreasing toward the middle of the basin. Chaotic reflectors are interpreted as sill intrusions. The thickness of the sill is difficult to determine as no coherent reflectors can be identified beneath the top contact. The sill underlies a more coherent package of reflectors, which is a few hundred meters thick in the deepest part of the basin.

the middle segment of the SUDB, however, shows the opposite sense of dip with outward facing faults common.

[20] In a region at 29.9°N, 113.3°W, centered in the middle of the Gulf (Foldout 3b; CDP 22000, line 25), a zone of closely spaced faults (~1 km apart) with opposing dips is associated with tilted strata. Evidence of erosional truncation in this area suggests that the strata were once domed up or tilted and exposed subaerially.

4.4. Wagner and Consag Basins

[21] Fault scarps are smaller and less common than in the other major basins (Figure 9), but the density of faults is higher in the WB than in the Upper Delfín Basins (Figure 4). Opposing fault dips are common in the axial region of the WB. There are many steeply dipping faults and a wide range of fault dips (Figure 4). The structural pattern is asymmetric, with more active faults over a broader region in the SE flank of the basin and a narrower, less active fault zone in the NW side of the basin. The sedimentary package imaged in the area of the WB is at least 2 km thick; PEMEX wells W1 and W3 (Figure 1b) penetrated 3 km or more of Pleistocene sediments, below which the ages were either undetermined (W3) or still Pleistocene (W1). The thick Pleistocene sediments are faulted downward into the WB along normal faults with seafloor offsets averaging just a few meters. The Consag Basin (Figure 10) to the south is generally shallower than the WB and may be a pull-apart in the left-stepping system of transform faults in the northern Gulf.

5. Delineation of the Major Rift Basins

[22] Isopach maps were used to identify the major active rift basins or depocenters in the northern Gulf (Figure 11). Because of the high density of faulting and disruption by igneous material, regional unconformities were not traceable throughout the major basins. We therefore chose a prominent reflector with good lateral continuity as the base of the youngest sediments. The thickness of the youngest sedimentary layer was then calculated by subtracting the thickness of the water column in two-way travel time. A velocity of 2000 m/s was used for the sediments to convert

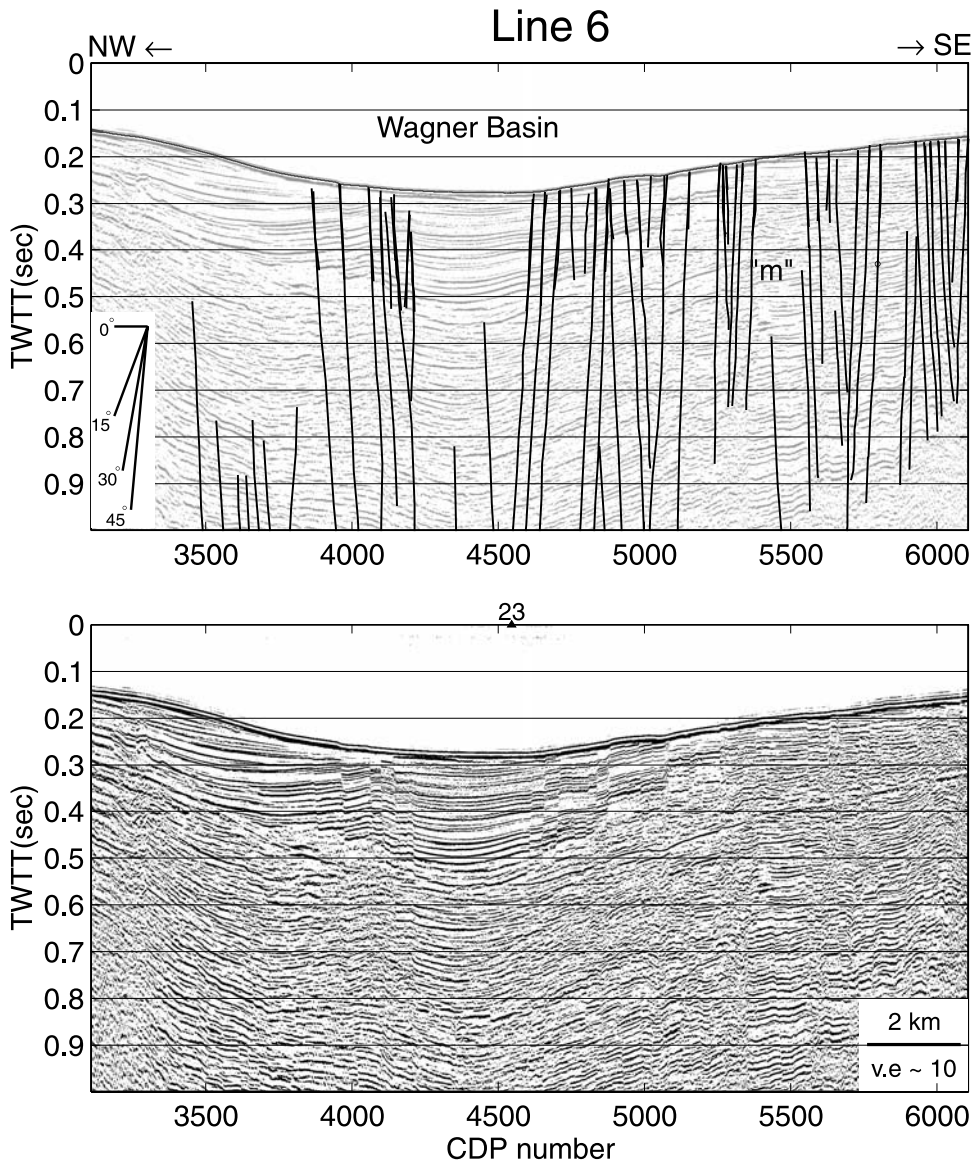

Figure 9. Seismic profile across the axis of the Wagner Basin. The sediment thickness is large here due to the high flux from the Colorado River located to the north. Note the high density of faults and their asymmetric distribution with respect to the center of the basin; more active faults are present on the SE side than on the NW side.

to thickness. The 150 m isopach was used to map the active basins (red lines in Figure 11).

[23] The trough of the LDB is outlined by the 800 m bathymetric contour. On the basis of the bathymetry, the basin trends N25°E. The 150-m isopach gives a length of 30 km and trend of N10°E. The LDB abuts the Ballenas transform to the SW, where it merges with the Salsipuedes Basin (Figure 1b), the deepest of all of the northern Gulf basins. Because of the partial coverage, reliable isopach maps could not be produced for the Salsipuedes Basin. The sedimentary package in the LDB is disrupted in many places by intrusions. The isopach map, however, clearly shows the segmentation of the LDB into two depressions (Figure 11) as is also observed in a seismic profile along the axis of the basin (Foldout 1a). An additional small depocenter, just north of the two depressions, is interpreted as a structural continuation of the LDB or another possibly younger segment of the basin (Figure 11).

[24] The southern boundary of the Upper Delfín Basins is located ~30 km northwest of the LDB. On the basis of the bathymetric data, the NUDB and SUDB are two subparallel basins of similar size. Seafloor relief in these basins is not as pronounced as in the LDB. A low of 400–450 m depth marks the SUDB, while the NUDB has maximum water depths of 300–350 m. Both basins are segmented and trend N35°E based on bathymetry and the 150 m isopach (Figures 1b and 11). The isopach maps give lengths of 50 km and 60 km for NUDB and SUDB, respectively, and show the NUDB and SUDB as an irregularly shaped but mostly continuous basin, with a thicker sedimentary package in the center of the NUDB and the ends of the SUDB. This reflects the same structural connections suggested by active faulting.

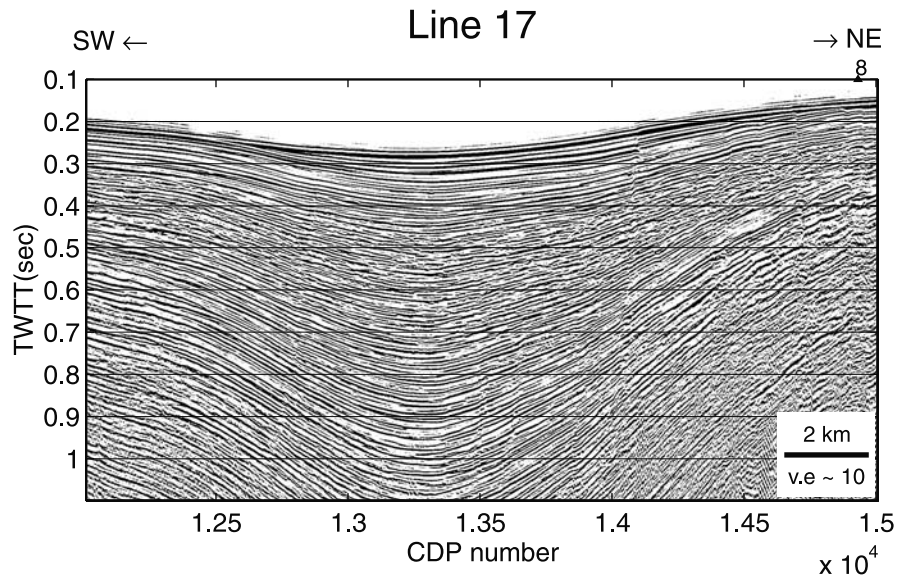

Figure 10. Uninterpreted seismic profile across the Consag Basin. It shows a large sediment-filled sag with very little faulting. This structure may be an accommodation zone.

[25] Interestingly, the youngest layer is thickest in the Consag Basin (CB) (Figure 11). Similarly, from the 150 m isopach, this basin appears to be broader than the WB to the north. The axes of these basins are ~15 km apart and the CB lies ~30 km northwest of the northern boundary of the NUDB. Water depths in the CB and WB are less than 250 m (Figure 1b). The WB trends N15°E–N20°E (Figure 1b) based on bathymetry and N12°E based on the 150 m isopach (Figure 11). It has a length of 13 km. On the basis of seismic profiles and heat flow data, the WB has been interpreted either as a bend along a transform fault, or a transform fault with another spreading center located to the north [*Henyey and Bischoff*, 1973]. This contrasts with a geologic-tectonic interpretation of this basin as an active spreading center [*Fenby and Gastil*, 1991].

6. Relationship Between Magmatism and Deformation

[26] The Lower Delfín Basin is magmatically the most active basin of those we surveyed. Along strike, the deepest part of the LDB is sandwiched between extrusive volcanic rocks to the northeast and the Baja California continental block to the southwest (Foldout 1a, line 64). The axis of the LDB is intruded by volcanic rocks, which form small knolls on the seafloor (Figures 2 and 3). Intrusive bodies and volcanic knolls are elongate along the axis of the LDB, but are narrow across axis (see star in Foldout 1). Compared to the LDB, the NUDB and SUDB have fewer volcanic knolls. One of these is the large knoll located in the southwest segment of the SUDB (Figure 2 and Foldout 1c), which produced dredge samples of rhyolite pumice [*Henyey and Bischoff*, 1973]. Sills are, however, not uncommon, particularly in the deeper parts of these basins, where chaotic reflectors underlie a coherent package of sediments (e.g., Figure 8 and Foldout 3a, line 56). The tops of sill bodies were interpreted and the depths are shown in Figure 12. There seems to be some correlation between shallow sills, recent extrusive volcanism, high *P* wave velocities and faulting (Figure 12). The one notable exception is the relatively large volcanic knoll in the southwest segment of the SUDB (Foldout 1c, CDP 10000), which is associated with a velocity low.

[27] Although no volcanic knolls were identified in the area of the WB, Consag Rock (Figure 1b), a small volcanic island west of the WB, may provide evidence for continued magmatic activity northward. Alternatively, it may be a remnant of older volcanic rock, such as the prerift andesite from the early to middle Miocene volcanic arc found in the adjacent area of Baja California [*Gastil et al.*, 1979]. The lack of identified extrusive and intrusive magmatism in the northern part of our survey may have resulted from the reduced ratio of igneous to sedimentary rock as the Colorado River delta is approached and the sedimentary column thickens, making this identification more difficult.

7. Basement

[28] If the northern Gulf crust is new igneous material, one would expect any extended continental basement to be restricted to the margins of the Gulf and not underlie the entire survey area. Indeed, the acoustic basement in the top 2 km of the crust can only be mapped at certain locations to within a few kilometers of the Baja California coastline. The basement is imaged in a seismic profile directly offshore of Volcán Prieto, approximately 10 km from the Baja Peninsula coastline (Figure 1b and Foldout 1c, line 62) and has an apparent dip of 4–5° southeastward into the Gulf. Just north of this profile, the basement depth increases from ~0.63 s TWTT (630 m at a seismic velocity of 2000 m/s) close to the Baja Peninsula to >1500 m at ~10 km away from the coastline, which may indicate an apparent northeastward dip also (Foldout 3a, line 56). Further evidence for a northeastward dip is the depth of 2800 m to the altered andesite in the W2 well located to the north (Figure 1b). We correlate the acoustic basement with the altered andesite rather than with the quartz-rich diorite at 2950 m in the W2 well. This correlation suggests that the

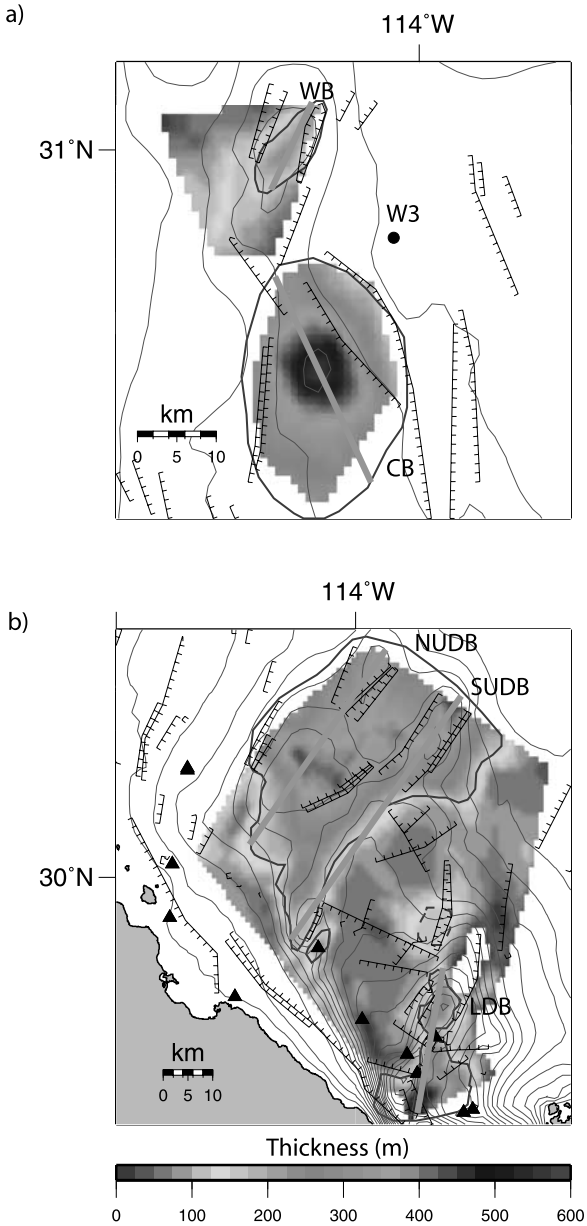

Figure 11. Isopach maps of the youngest sediments in (a) the Wagner and Consag Basins and (b) the Upper Delfín and Lower Delfín Basins. Thickness is given in meters below the seafloor. A velocity of 2000 m/s was used to convert TWTT to thickness. Solid red lines outline the major basins/depocenters. Thick gray lines represent the axes of the basins. These are based on the 150 m isopach. An additional small depocenter with no bathymetric expression is also shown (dashed red line). CB, Consag Basin; LDB, Lower Delfín Basin; NUDB, Northern Upper Delfín Basin; SUDB, Southern Upper Delfín Basin; W3, PEMEX well. See color version of this figure at back of this issue.

dip of the basement from the profile shown in Foldout 1a (line 56) to W2 is ~5°. Fitting a plane to all of the basement depths interpreted in the reflection data gives a N–S strike and true dip of 5.2°E. This estimate supports the idea of a basement with relatively uniform dip and some local structure. The basement surface appears to be somewhat irregular and may indeed be affected by faulting; however, no large offset (>0.1 s TWTT) normal faults were interpreted in this area. Deciphering any lateral offsets of the basement is not presently possible.

[29] Limited constraints on the composition of the deeper basement in the northern Gulf come from the sonobuoy data. From the analysis of refraction data, *Phillips* [1964] identified igneous and metamorphic basement with a seismic velocity of 5.53 km/s at a depth of ~4 km in the northern Gulf. In addition, shallow magnetic horizons have been estimated at depths of 2.3–4.1 km below sea level [*Sánchez-Zamora et al.*, 1991]. Our refraction data show a large jump (1 km/s or more) associated with every velocity change to ~5.0 km/s. We interpret velocities >5.0 km/s as basement, possibly containing some amount of sedimentary material similar to that found in the Guaymas Basin [*Einsele et al.*, 1980].

[30] Velocity highs seen at shallow depths (1.2 km) close to Gonzaga Bay and 30.2°N, −113.8°W are correlated with volcanic protrusions on the seafloor (Figure 13). The shooting tracks of the sonobuoys did not traverse every volcanic knoll in the area (e.g., those close to Isla Angel de la Guarda in the LDB do not all have sonobuoy coverage), and we therefore cannot determine whether or not they all are associated with high velocities (Figure 13). Above 2 km, with the exception of the higher velocities in San Luis Gonzaga Bay, the velocities are ≤3.5 km/s (Figure 13). The

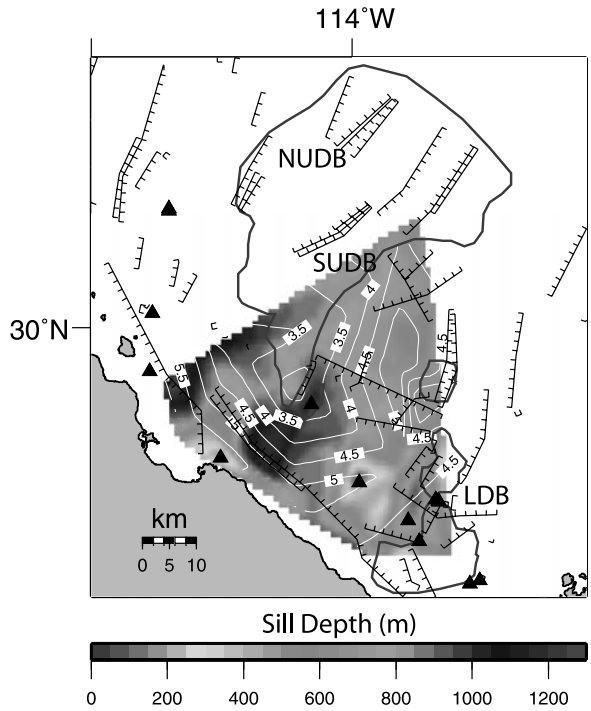

Figure 12. Map showing sill depth in meters below the seafloor overlain by contours (white lines) of *P* wave velocities at 2.8 km depth below the sea surface. Contours are shown at 0.5 km/s intervals. The sill depths shown are for multiple sills and represent an interpolation between different bodies. The major basins are outlined in red, based on the 150-m isopachs shown in Figure 11. Triangles are volcanic knolls. See color version of this figure at back of this issue.

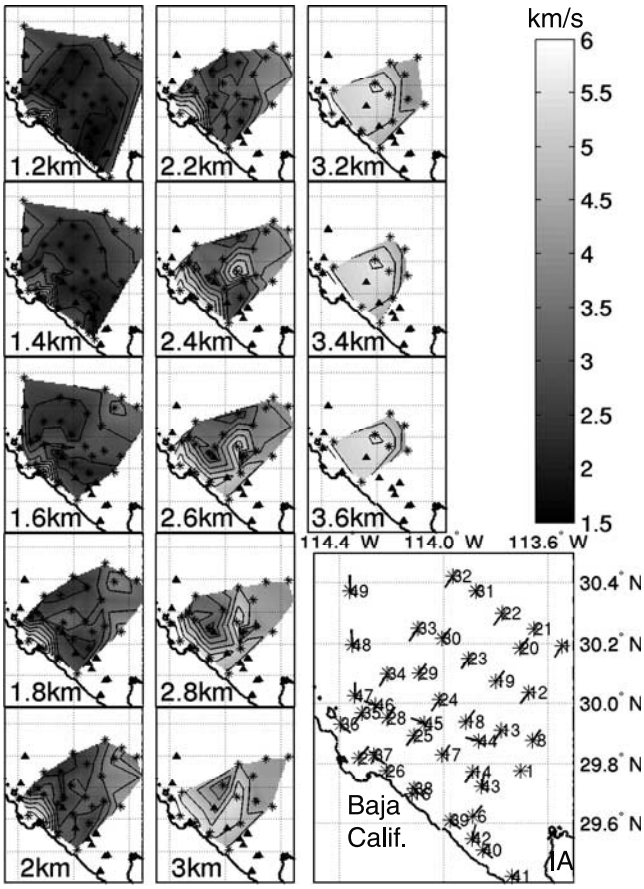

Figure 13. Depth slices showing interval velocities in the northern Gulf of California. Black triangles are volcanic knolls and gray stars mark the sonobuoy locations with tails pointing in the direction in which the ship was travelling. In each depth slice, the gray stars show the sonobuoys with data at that depth. IA, Isla Angel de la Guarda. See color version of this figure at back of this issue.

fairly smooth increase in velocities with depth suggests a thick sequence of unconsolidated to consolidated sediments (Figure 13). At depths larger than 2 km, sonobuoys 14, 18, 24, 27, 35, 36 and 38 show basement velocities greater than ~5 km/s. At the location of sonobuoy 36, basement velocity is 6.4 km/s. This is close to the Baja California coast and is probably volcanic basement similar to the basaltic andesites to rhyolites found in the nearby Holocene volcanic center of Isla San Luis [*Paz Moreno and Demant*, 1999]. The higher velocities between the middle segment of the SUDB and the LDB may indicate less extended igneous/metamorphic crust and a thinner sedimentary package between these basins.

8. Discussion

[31] The northern Gulf of California displays a complex structural pattern which will be discussed in the context of onshore versus offshore faulting, rift obliquity and the transition to seafloor spreading.

8.1. Onshore Versus Offshore Faulting

[32] Here, we compare the offshore faults to the onshore structure of northeastern Baja California east of the Sierra San Pedro Mártir, between San Felipe (31°N) and Gonzaga Bay (29.8°N), where the spatial and temporal development of faulting is well established.

8.1.1. Synthesis of Offshore Structure

[33] On the basis of our interpretation of the seismic data, faulting in the northern Gulf of California occurs over a broad depressed region, approximately 70 × 200 km encompassing multiple rift basins. Our map shows a broad zone of deformation, comprised of many oblique-slip faults with true dips of ~60–80° and varying azimuths (Figure 4). No primary or throughgoing structures such as transform faults were identified in the northern Gulf. In the axial regions of the Upper Delfín Basins, most faults are NE striking normal faults with some lateral offset. The Lower Delfín Basin has two mutually crosscutting sets of active faults (NE striking normal and NW striking oblique-normal faults) (Figure 14a). NW striking, oblique-normal faults parallel the Baja California coastline. The uplifted zone north of Isla Angel de la Guarda may have accommodated extension created by listric ramp-flat faulting at depth. In the area of the Wagner and Consag Basins, faults generally strike northerly. We expect the Wagner Basin originated as part of an older extensional domain bounded by a major strike-slip fault located NE of Isla Angel de la Guarda, perhaps even outside of our survey area. We hypothesize that the orientation of the extensional component of this system was not significantly different than it is at present, since the Wagner Basin is still a major part of the plate boundary.

[34] The overall shallow structure in the northern Gulf is that of a pull-apart basin containing at least three major extensional domains or duplexes, the LDB, SUDB and NUDB. Extensional duplexes are known to form at releasing bends or offsets along strike-slip faults and on straight strike-slip faults [*Woodcock and Fischer*, 1986]. These duplexes appear to merge with transtensional branches from the BTF, forming a horsetail structure (Figure 14b). This indicates a transtensional fault zone NW of Isla Angel de la Guarda, where the small volcanic knolls are concentrated. This broad pull-apart basin is floored by basement of mixed igneous-sedimentary material, within which some blocks of older continental crust may exist. Structurally, the northern Gulf does not look like a typical mid-ocean ridge environment. There are no "ridges" and seafloor spreading is still not occurring.

8.1.2. Synthesis of Onshore Structure

[35] We found no evidence for a continuation of the present onshore structures into the offshore in the northern Gulf. In contrast to the style of faulting in the offshore, onshore deformation consists of two structural regimes separated by the Puertecitos Volcanic Province (PVP) (domains II and III in Figure 14) and bounded to the west by the Main Gulf Escarpment (domain I) [*Dokka and Merriam*, 1982]. A well-developed basin and range topography with east dipping listric normal faults developed between 12 and 6 Ma north of the PVP in domain II [*Dokka and Merriam*, 1982; *Stock and Hodges*, 1990], suggesting a period of E-W extension. Interpretation of kinematic data inversions along with published paleomagnetic data provide evidence for a W-E and SW-NE orientation of the axis of least principal stress in late Miocene time [*Lewis and Stock*, 1998b]. Sometime after 6 Ma the style of faulting in NE

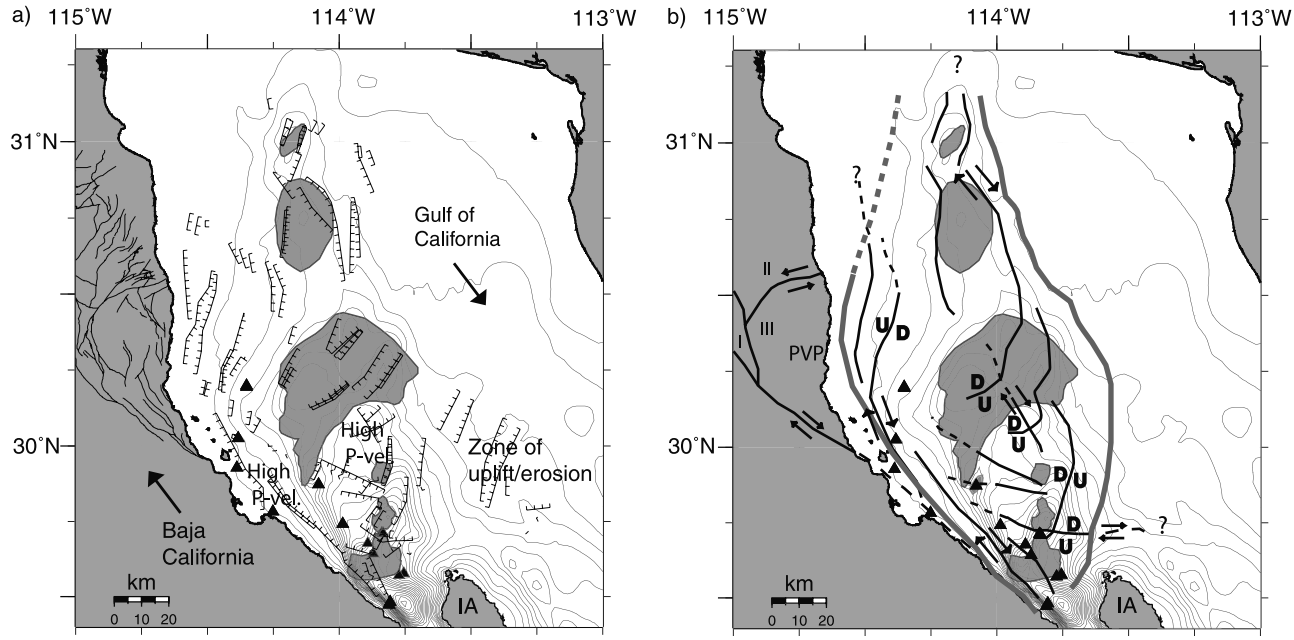

Figure 14. (a) Summary map showing the faults interpreted in our reflection data (black lines with hachures on the downthrown side), bathymetric contours every 50 m (thin gray lines), the major basins determined from the 150 m isopach (gray fill) and areas of high *P* velocities from our refraction data. Heavy black arrows indicate the current Pacific-North America relative plate motion direction, N37°W [*Atwater and Stock*, 1998]. Onshore faults are from *Oskin et al.* [2001]. (b) Schematic drawing summarizing the major tectonic elements identified in the northern Gulf. The onshore structural domains (I, II, and III) are after *Dokka and Merriam* [1982]. Black lines offshore represent the extensional strands of a broad shallow basin (outlined by thick gray lines) and faults that cut across the axis of the LDB. Arrows represent the sense of lateral slip. "U" and "D" refer to the sense of vertical slip. Solid triangles are volcanic knolls. See text for discussion. PVP, Puertecitos Volcanic Province; IA, Isla Angel de la Guarda.

Baja California east of the rift margin, east of the San Pedro Mártir border fault, changed to E-W extension [*Dokka and Merriam*, 1982]. Pliocene to Recent extension along the western rift margin of the GEP remained E–NE directed [*Nagy and Stock*, 2000]. At about 3 Ma, extension within the Gulf Extensional Province was approximately oriented WSW-ENE [*Lewis and Stock*, 1998b] and NE striking faults were rotated and reactivated with sinistral slip [*Lewis and Stock*, 1998a]. These faults have accommodated an average of 30° of clockwise rotation of late Miocene tuffs around vertical axes [*Lewis and Stock*, 1998a]. In domain III, south of Puertecitos there are no major NE striking sinistral faults. A series of mostly <6.3 Ma, NW-NNW striking, down-to-the-east, high-angle, normal faults exists between the PVP and Gonzaga Bay [*Oskin*, 2002, Chapter 6; *Stock and Hodges*, 1990; *Stock*, 2000].

[36] In domain I, the active (Holocene) San Pedro Mártir fault, at the western margin of the Gulf Extensional Province north of the PVP records 5 km of vertical separation [*Brown*, 1978]. No evidence has been found for such large offsets on a single fault in the offshore. In order to image such offsets, deeper seismic data are required.

8.1.3. Comparison of Onshore and Offshore Structure

[37] Limited by the fact that our data do not penetrate the middle and lower crust, the present NE striking onshore faults largely appear to terminate near the shoreline and are apparently not continuous out into the northern Gulf. Deformation in the shallow crust in the northern Gulf appears to be occurring in a different manner to that observed onshore within the continental extensional province. We speculate that the offshore structures may reflect a different and more recent stress regime than the onshore faults.

8.2. Influence of Rift Obliquity on Deformation

[38] The angle, α, between the plate motion direction, N37°W [*Atwater and Stock*, 1998], and the rift trend or plate margin in the Gulf of California is approximately 20° or 30° [*Withjack and Jamison*, 1986]. Although obliquity can be locally related to different mechanisms such as excess magma injection compared to far field forces as in the case of Reykjanes Ridge [*Abelson and Agnon*, 1997], in this discussion we assume that obliquity is only a result of plate motion and hence, does not vary along the axis of the Gulf. Theory [*Fossen and Tikoff*, 1993] and kinematic modeling [*Teyssier et al.*, 1995] have shown that strike-slip partitioning in continental crust is higher for higher rift obliquities (i.e., smaller α) and wrench-dominated transtension occurs for $\alpha \leq 20°$. The fault pattern in the northern Gulf, however, suggests a limited degree of strike-slip partitioning, where faults with a larger/obvious strike-slip component are concentrated close to the Baja California coast and faults with a dominantly extensional component are concentrated in the middle of the rift. Most of the faults

are, however, interpreted as having oblique slip rather than purely strike or dip slip, indicating incomplete strain partitioning.

[39] Scaled analog experiments on displacement partitioning in basins and the lithosphere have shown that a viscous ductile layer at depth is needed to produce strike-slip partitioning during transpression [*Richard and Cobbold*, 1990]. This viscous ductile layer decouples the upper crust from the zone of shear at depth. In the absence of this layer, oblique slip faults will form instead of either purely strike-slip or purely dip-slip faults [*Richard and Cobbold*, 1990] because the transmission of basal shear forces to the upper and middle crust is more efficient. Strike-slip partitioning in the northern Gulf is incomplete. We suggest, therefore, that the lower crust in the northern Gulf of California is relatively thin or strong, the latter implying it is mantle derived.

[40] From analog experiments it is also known that the range of azimuths in a fault population should increase as rift obliquity increases (i.e., α decreases), with two orientations first becoming predominant at $\alpha \leq 30°$: one approximately rift parallel and the other displacement normal [*Clifton et al.*, 2000]. For these obliquities, faults that develop within the rift have dip-slip, oblique-slip and strike-slip motion [*Clifton et al.*, 2000]. Our observations in the northern Gulf of a predominantly rift-parallel fault population and overall large variations in fault orientations and dips partly confirm the results of analog models (Figure 4).

[41] In addition, the rift basins are oriented approximately perpendicular to N37°W, the plate motion direction [*Atwater and Stock*, 1998], in the deepest parts of the northern Gulf, but oblique to the plate motion direction in the shallower areas. There are no large basin-bounding faults or well-defined zones of strike-slip or normal faulting. These structural styles are typical of mechanical models of oblique rifts. *Mart and Dauteil* [2000] showed that during analog experiments with rift obliquities of 15°, undulating rifts formed with central diapirs separated by threshold zones of diffuse extension.

[42] Numerical results of purely strike-slip deformation in a pull-apart basin driven from below show that a wider basal shear zone produces a broader, longer and shallower zone of surface deformation [*Katzman et al.*, 1995]. By adding a small component of extension, a large component of regional subsidence is produced [*ten Brink et al.*, 1996]. On the basis of the fact that brittle deformation in the northern Gulf is occurring by multiple small-offset faults in a broad zone of deformation, we also expect the basal shear zone beneath the crust to be wide. The fact that no local heat flow highs were identified in the northern Gulf [*Henyey and Bischoff*, 1973; *Sánchez-Zamora et al.*, 1991] also supports a broad shear zone at depth.

8.3. Transition to Seafloor Spreading

[43] If both the southern and northern parts of the Gulf have experienced the same amount of opening, why is there still no seafloor spreading in the northern part? Is it because of heterogeneities in thinning of the crust along the axis of the Gulf, or differences in initial crustal composition or physical properties such as crustal thickness and strength? Although a comparison with the southern Gulf is beyond the scope of this work, our results illuminate two points in which the northern and southern parts of the Gulf differ: (1) strain partitioning and (2) sediment thickness.

[44] It has been suggested that the temporal overlap of 3–4 m.y. between continental rifting and seafloor spreading in the Gulf resulted from its obliquity [*Fletcher and Munguia*, 2000]. The overall structure of the Gulf of California is a series of long transform faults and short spreading centers. This geometry keeps the continental crust weak by dragging it past the spreading centers while suppressing active asthenospheric upwelling by cooling of the spreading center through lateral heat transfer to the continental crust; this prolongs the period of normal faulting in continental crust and increases interplate coupling [*Fletcher and Munguia*, 2000].

[45] Although these arguments may apply to the southern and central parts of the Gulf, the absence of long transform faults in the northern Gulf requires a different mechanism for the long-lived continental rifting and the delay in the transition to seafloor spreading in this region. The northern Gulf has a complex fault system consisting of multiple oblique-slip faults over a broad area versus the transform fault spreading center geometry of the southern Gulf. The former is likely to transfer less heat to the continental crust than the latter; therefore any mechanism that distributes deformation in the northern Gulf and consequently slows the transition to seafloor spreading must also allow for an extended period of rifting in the continental crust unrelated to the structural geometry of the adjacent plate boundary. We suggest a broad zone of basal shear in the northern Gulf coupled with its inherent obliquity causes strain to be spatially distributed and the degree of strike-slip partitioning to be small. Deformation on the margins of the northern Gulf is thus maintained on two widely separated fault systems, the transpeninsular faults which merge into the Gulf Extensional Province and the Cerro Prieto transform fault. We further speculate that the westward jumps in extension in the northern Gulf over the last several million years may be related to the interaction of these two fault systems.

[46] The delay in the transition to seafloor spreading in the northern Gulf may also be controlled by the higher sediment flux from the Colorado River [e.g., *Einsele*, 1986]. Deposition of cold sediments has an initial cooling effect. In the long term, however, a thick blanket of low thermal conductivity sediments acts as an insulator and inhibits the localization of deformation by keeping the crust equally weak everywhere. Thick porous sediments also facilitate the intrusion of sills [*Einsele et al.*, 1980; *McBirney*, 1963; *Saunders et al.*, 1982] rather than dikes, which would be needed for the development of a typical mid-ocean ridge.

9. Conclusions

[47] The plate boundary in the northern Gulf of California is a wide zone of oblique faulting. Our results show a broad shallow basin, approximately 70 × 200 km with six 10-km-scale subbasins spaced 15 or 30 km apart: an L-shaped depression (LDB and Salsipuedes Basin), two subparallel rift basins (NUDB and SUDB) and a possible accommodation zone comprised of the WB and CB. All basins are segmented along axis. With the exception of the Salsipuedes Basin, they all trend oblique to the plate motion direction. There are no

clear structural connections such as transform faults between these three groups of basins; however, each group is morphologically distinct and the basins in each group show similarities in fault systematics and magmatism. Based on magmatic and fault activity, the LDB is the most active of the basins surveyed. Most of the faults in the survey have apparent dips of $\sim 50-60^\circ$ suggesting that the plate boundary is made up of mainly oblique-normal faults. Major faults have true dips of $\sim 70^\circ$. In general seafloor scarps are smaller in the northern part of the survey area (e.g., WB) than in the southern part (e.g., LDB), reflecting the influence of a higher sediment flux closer to the Colorado River delta. Fault density in the WB is, however, as high as in the LDB. From this we conclude that although it is likely that true seafloor will first be produced in the LDB based on the near-surface manifestations of active magmatism and faulting, the WB plays a significant and perhaps major role in active deformation in the northern Gulf.

[48] Our reflection equipment imaged the top 2 km of the sedimentary package, which may be no older than Pleistocene in age, perhaps with some Pliocene in the lowest part we image. Throughout the area surveyed, our data show many faults spaced a few kilometers apart, with small offsets. There are no major faults that take up most of the extension. The northern Gulf consists of a complex network of predominantly NE striking normal faults dissected in part by NW striking oblique-normal faults. Some of the faults observed in the shallow crust may merge at depth into single fault planes with larger cumulative offset. On the basis of sonobuoy data, PEMEX well data and reflection profiles, the basement dips 5° E-SE adjacent to NE Baja California. A zone of predominantly strike-slip deformation lies along the peninsular coast (Figure 14), where some faults penetrate basement. This zone marks the northern extent of the Ballenas Transform Fault zone but does not contain a simple transform fault. Volcanic knolls are located either along the transform fault zones or within the rifts close to these zones. This suggests that the transform fault is transtensional. The NW end of the Ballenas transform fault branches off into multiple rift basins forming a horsetail structure (Figure 14). The rift basins of the northern Gulf represent many strands of the transform fault zone, which clearly possesses a tensional component north of Isla Angel de la Guarda. This is first expressed in the deep Salsipuedes Basin. Moving from the LDB to the Upper Delfín Basins, the transform fault loses offset with each additional rift. It becomes increasingly difficult to identify discrete zones of strike-slip offset.

[49] We found no evidence for a continuation of the onshore structures into the offshore and fewer throughgoing structures than previous workers. On the basis of the fact that mainly oblique slip faults are present and active, we conclude that strike-slip partitioning is incomplete. The style of deformation we image may have resulted from shear at depth beneath a strong lower crust that effectively transmits the oblique stresses to the weaker upper crust.

[50] It is likely that the early stages of rifting elsewhere closely resemble the current deformation in the northern Gulf, where wide zones of lower lithospheric shear, rift obliquity, sediment flux, crustal thickness and rheology influence the focusing of deformation within the rift. We have shown that deformation is distributed in the northern Gulf and suggest that this is typical of young oblique rifts. We further suggest that sediment supply plays a significant role in keeping deformation distributed.

[51] **Acknowledgments.** We thank the captain and the crew of the B/O *Francisco de Ulloa*, as well as Peter Buhl, Sergio Paz, Jose Luis Garcia Puga, and Erich Scholz for making the data collection process successful. We are extremely grateful to Joyce Alsop for her invaluable help and support in processing the seismic data. We thank Julie Nazareth for reviewing early drafts of this manuscript and Uri ten Brink along with two anonymous reviewers for providing thorough reviews of the submitted manuscript, though we remain solely responsible for the ideas contained herein. This research was supported by US National Science Foundation grants OCE-9730790 to Caltech and OCE-9730569 to LDEO, and by CONACYT grant 26669-T to CICESE. We thank PEMEX Exploración y Producción for the permit to use the well data from the northern Gulf of California. Contribution 8863, Division of Geological and Planetary Sciences, California Institute of Technology. Lamont-Doherty Earth Observatory contribution 6385.

References

Abelson, M., and A. Agnon, Mechanics of oblique spreading and ridge segmentation, *Earth Planet. Sci. Lett.*, *148*, 405–421, 1997.

Aragón-Arreola, M., A. Martín-Barajas, and J. M. Stock, Estructura y evolución de las cuencas fósiles en el norte del Golfo de California a partir de sísmica de reflexión multicanal, *GEOS*, *22*, 181, 2002.

Atwater, T., and J. Stock, Pacific-North America Plate tectonics of the Neogene southwestern United States: An update, *Int. Geol. Rev.*, *40*, 375–402, 1998.

Badley, M. E., *Practical Seismic Interpretation*, Int. Human Resour. Dev. Corp., Boston, Mass., 1985.

Barker, D. H., Rift propagation, detachment faulting, and associated magmatism in Bransfield Strait, Antartica Peninsula, *J. Geophys. Res.*, *103*, 24,017–24,043, 1998.

Bennett, R. A., W. Rodi, and R. E. Reilinger, Global Positioning System constraints on fault slip rates in southern California and northern Baja, Mexico, *J. Geophys. Res.*, *101*, 21,943–21,960, 1996.

Bischoff, J. L., and T. L. Henyey, Tectonic elements of the central part of the Gulf of California, *Geol. Soc. Am. Bull.*, *85*, 1893–1904, 1974.

Boillot, G., D. Mougenot, J. Girardeau, and E. L. Winterer, Rifting processes on the West Galicia Margin, Spain, in *Extensional Tectonics and Stratigraphy of the North Atlantic Margins*, edited by A. J. Tankard and H. R. Balkwill, *AAPG Mem.*, *46*, 363–377, 1989.

Brown, L. G., Recent fault scarps along the eastern escarpments of the Sierra San Pedro Mártir, Baja California, Masters thesis, San Diego State Univ., San Diego, Calif., 1978.

Clifton, A. E., R. W. Schlische, M. O. Withjack, and R. V. Ackermann, Influence of rift obliquity on fault-population systematics: Results of experimental clay models, *J. Struct. Geol.*, *22*, 1491–1509, 2000.

Cochran, J. R., and F. Martinez, Evidence from the northern Red Sea on the transition from continental to oceanic rifting, *Tectonophysics*, *153*, 25–53, 1988.

Couch, R. W., G. E. Ness, O. Sanchez-Zamora, G. Calderón-Riveroll, P. Doguin, T. Plawman, S. Coperude, B. Huehn, and W. Gumma, Gravity anomalies and crustal structure of the Gulf and Peninsular Province of the Californias, in *The Gulf and Peninsular Provinces of the Californias*, edited by J. P. Dauphin and B. R. T. Simoneit, *AAPG Mem.*, *47*, 25–45, 1991.

Curray, J. R., D. G. Moore, L. A. Lawver, F. J. Emmel, R. W. Raitt, M. Henry, and R. Kieckhefer, Tectonics of the Andaman Sea and Burma, in *Geological and Geophysical Investigations of Continental Margins*, edited by J. S. Watkins, L. Montadert, and P. W. Dickerson, *AAPG Mem.*, *29*, 189–198, 1979.

DeMets, C., A reappraisal of seafloor spreading lineations in the Gulf of California: Implications for the transfer of Baja California to the Pacific plate and estimates of Pacific-North America plate motion, *Geophys. Res. Lett.*, *22*, 3545–3548, 1995.

Dokka, R. K., and R. H. Merriam, Late Cenozoic extension of northeastern Baja California, Mexico, *Geol. Soc. Am. Bull.*, *93*, 371–378, 1982.

Driscoll, N. W., and G. D. Karner, Lower crustal extension across the Northern Carnarvon Basin, Australia: Evidence for an eastward dipping detachment, *J. Geophys. Res.*, *103*, 4975–4991, 1998.

Einsele, G., Interaction between sediments and basalt injections in young Gulf of California-type spreading centers, *Geol. Rundsch.*, *75*, 197–208, 1986.

Einsele, G., et al., Intrusion of basaltic sills into highly porous sediments and resulting hydrothermal activity, *Nature*, *283*, 441–445, 1980.

Fenby, S. S., and R.G. Gastil, Geologic-tectonic map of the Gulf of California and surrounding areas, in *The Gulf and Peninsular Provinces of the Californias*, edited by J. P. Dauphin and B. R. T. Simoneit, *AAPG Mem.*, *47*, 79–83, 1991.

Fletcher, J. M., and L. Munguia, Active continental rifting in southern Baja California, Mexico: Implications for plate motion partitioning and the transition to seafloor spreading in the Gulf of California, *Tectonics*, *19*, 1107–1123, 2000.

Fossen, H., and B. Tikoff, The deformation matrix for simultaneous simple shearing, pure shearing and volume change, and its application to transpression-transtension tectonics, *J. Struct. Geol.*, *15*, 413–422, 1993.

Frez, J., and J. J. González, Crustal structure and seismotectonics of northern Baja California, in *The Gulf and Peninsular Provinces of the Californias*, edited by J. P. Dauphin and B. R. T. Simoneit, *AAPG Mem.*, *47*, 261–283, 1991.

Fuis, G. S., and W. M. Kohler, Crustal structure and tectonics of the Imperial Valley region, California, in *The Imperial Basin-Tectonics, Sedimentation and Thermal Aspects*, edited by A. C. Rigsby, pp. 1–13, Pac. Sect., Soc. for Sediment. Geol., Los Angeles, Calif., 1984.

Gastil, R. G., D. Krummenacher, and J. Minch, The record of Cenozoic volcanism around the Gulf of California, *Geol. Soc. Am. Bull.*, *90*, 839–857, 1979.

Goff, J. A., E. A. Bergman, and S. C. Solomon, Earthquake source mechanisms and transform tectonics in the Gulf of California, *J. Geophys. Res.*, *92*, 10,485–10,510, 1987.

González-Fernández, A., J. J. Danobeitia, D. Córdoba, L.A. Delgado-Argote, R. Carbonell, and R. Bartolomo, Estructura de la litósfera en el alto Golfo de California a partir de datos de sísmica de reflexion multicanal, sísmica de granángulo y gravimetría, *GEOS*, *19*, 219, 1999.

Harding, T. P., Identification of wrench faults using subsurface structural data: Criteria and pitfalls, *AAPG Bull.*, *74*, 1590–1609, 1990.

Helenes, J., and A. L. Carreño, Neogene sedimentary evolution of Baja California in relation to regional tectonics, *J. S. Am. Earth Sci.*, *12*, 589–605, 1999.

Henry, C. D., and J. J. Aranda-Gómez, Plate interactions control middle-late Miocene, proto-Gulf and Basin and Range extension in the southern Basin and Range, *Tectonophysics*, *318*, 1–26, 2000.

Henyey, T. L., and J. L. Bischoff, Tectonic elements of the northern part of the Gulf of California, *Geol. Soc. Am. Bull.*, *84*, 315–330, 1973.

Herman, B. M., R. N. Anderson, and M. Truchan, Extensional tectonics in the Okinawa Trough, in *Geological and Geophysical Investigations of Continental Margins*, edited by J. S. Watkins, L. Montadert, and P. W. Dickerson, *AAPG Mem.*, *29*, pp. 199–208, 1979.

Humphreys, E. D., and R. J. Weldon II, Kinematic Constraints on the Rifting of Baja California, in *The Gulf and Peninsular Provinces of the Californias*, edited by J. P. Dauphin and B. R. T. Simoneit, *AAPG Mem.*, *47*, 217–228, 1991.

Karig, D. E., and W. Jensky, The proto-Gulf of California, *Earth Planet. Sci. Lett.*, *17*, 169–174, 1972.

Katzman, R., U. S. ten Brink, and J. Lin, Three-dimensional modeling of pull-apart basins: Implications for the tectonics of the Dead Sea Basin, *J. Geophys. Res.*, *100*, 6295–6312, 1995.

Klitgord, K. D., J. D. Mudie, J. L. Bischoff, and T. L. Henyey, Magnetic anomalies in the northern and central Gulf of California, *Geol. Soc. Am. Bull.*, *85*, 815–820, 1974.

Larson, R. L., Bathymetry, magnetic anomalies, and plate tectonic history of the mouth of the Gulf of California, *Geol. Soc. Am. Bull.*, *83*, 3345–3360, 1972.

Lavier, L. L., W. R. Buck, and A. N. B. Poliakov, Factors controlling normal fault offset in an ideal brittle layer, *J. Geophys. Res.*, *105*, 23,431–23,442, 2000.

Lawver, L. A., J. G. Sclater, T. L. Henyey, and J. Rogers, Heat flow measurements in the southern portion of the Gulf of California, *Earth Planet. Sci. Lett.*, *12*, 198–208, 1973.

Lewis, C. J., and J. M. Stock, Paleomagnetic evidence of localized rotations during Neogene extension in the Sierra San Fermin, northeastern Baja California, Mexico, *J. Geophys. Res.*, *103*, 2455–2470, 1998a.

Lewis, C. J., and J. M. Stock, Late Miocene to Recent transtensional tectonics in the Sierra San Fermín, *J. Struct. Geol.*, *20*, 1043–1063, 1998b.

Lewis, J. L., S. M. Day, H. Magistrale, R. R. Castro, L. Astiz, C. Rebollar, J. Eakins, F. L. Vernon, and J. N. Brune, Crustal thickness of the Peninsular Ranges and Gulf Extensional Province in the Californias, *J. Geophys. Res.*, *106*, 13,599–13,611, 2001.

Lonsdale, P., Geology and tectonic history of the Gulf of California, in *The Geology of North America*, vol. N *The Eastern Pacific Ocean and Hawaii*, edited by D. Hussong, E. L. Winterer, and R. W. Decker, pp. 499–522, Geol. Soc. of Am., Boulder, Colo., 1989.

Manatschal, G., and D. Bernoulli, Architecture and tectonic evolution of nonvolcanic margins: Present-day Galicia and ancient Adria, *Tectonics*, *18*, 1099–1119, 1999.

Manighetti, I., P. Tapponnier, P. Y. Gillot, E. Jacques, V. Courtillot, R. Armijo, J. C. Ruegg, and G. King, Propagation of rifting along the Arabia-Somalia plate boundary: Into Afar, *J. Geophys. Res.*, *103*, 4947–4974, 1998.

Mart, Y., and O. Dauteil, Analogue experiments of propagation of oblique rifts, *Tectonophysics*, *316*, 121–132, 2000.

McBirney, A. R., Factors governing the nature of submarine volcanism, *Bull. Volcanol.*, *26*, 455–469, 1963.

McHargue, T. R., T. L. Heidrick, and J. E. Livingston, Tectonostratigraphic development of the interior Sudan rifts, central Africa, *Tectonophysics*, *213*, 187–202, 1992.

Molnar, P., Continental tectonics in the aftermath of plate tectonics, *Nature*, *335*, 131–137, 1988.

Nagy, E. A., and J. M. Stock, Structural controls on the continent-ocean transition in the northern Gulf of California, *J. Geophys. Res.*, *105*, 16,251–16,269, 2000.

Ness, G. E., M. W. Lyle, and R. W. Couch, Marine magnetic anomalies and oceanic crustal isochrons of the Gulf and Peninsular Province of the Californias, *The Gulf and Peninsular Provinces of the Californias*, edited by J. P. Dauphin and B. R. T. Simoneit, *AAPG Mem.*, *47*, 47–69, 1991.

Nicolas, A., Novel type of crust produced during continental rifting, *Nature*, *315*, 112–115, 1985.

Oskin, M., Tectonic evolution of the northern Gulf of California, Mexico, deduced from conjugate rifted margins of the upper Delfín Basin, Ph.D. thesis, Calif. Inst. of Technol., Pasadena, Calif., 2002.

Oskin, M., J. Stock, and A. Martin-Barajas, Rapid localization of Pacific-North America plate motion in the Gulf of California, *Geology*, *29*, 459–462, 2001.

Paz-López, S., Procesamiento e Interpretación de Datos Sísmicos y Gravimétricos en el Norte del Golfo de California, Masters Thesis, CICESE, Ensenada, Baja California, Mexico, 2000.

Paz Moreno, F. A., and A. Demant, The Recent Isla San Luis volcanic center: Petrology of a rift-related volcanic suite in northern Gulf of California, Mexico, *J. Volcanol. Geotherm. Res.*, *93*, 31–52, 1999.

Pérez-Cruz, G. A., Exploración Petrolera de la Porción Noroccidental del Golfo de California, *Bol. Asoc. Mex. Geofís. Explor.*, *21*, 81–128, 1980.

Phillips, R. P., Seismic refraction studies in Gulf of California, in *Marine Geology of the Gulf of California*, edited by T. van Andel and G. G. Shor, *AAPG Mem.*, *3*, 90–125, 1964.

Richard, P., and P. Cobbold, Experimental insights into partitioning of fault motions in continental convergent wrench zones, *Ann. Tectonicae, IV*, 35–44, 1990.

Sánchez-Zamora, O., P. Doguin, R. W. Couch, and G. E. Ness, Magnetic anomalies of the northern Gulf of California: structural and thermal interpretations, in *The Gulf and Peninsular Provinces of the Californias*, edited by J. P. Dauphin and B. R. T. Simoneit, *AAPG Mem.*, *47*, 377–401, 1991.

Saunders, A. D., D. J. Fornari, and M. A. Morrison, The composition and emplacement of basaltic magmas produced during the development of continental-margin basins: The Gulf of California, Mexico, *J. Geol. Soc. London*, *139*(3), 335–346, 1982.

Sawlan, M. G., Magmatic evolution of the Gulf of California Rift, in *The Gulf and Peninsular Provinces of the Californias*, edited by J. P. Dauphin and B. R. T. Simoneit, *AAPG Mem.*, *47*, 301–369, 1991.

Steckler, M. S., F. Berthelot, N. Lyberis, and X. Le Pichon, Subsidence in the Gulf of Suez: Implications for rifting and plate kinematics, *Tectonophysics*, *153*, 249–270, 1988.

Stock, J. M., Relation of the Puertecitos Volcanic Province, Baja California, Mexico, to development of the plate boundary in the Gulf of California, in *Cenozoic Tectonics and Volcanism of Mexico*, edited by H. Delgado-Granados, G. Aguirre-Díaz, and J. M. Stock, *Spec. Pap. Geol. Soc. Am.*, *334*, 143–156, 2000.

Stock, J. M., and K. V. Hodges, Pre-Pliocene extension around the Gulf of California and the transfer of Baja California to the Pacific plate, *Tectonics*, *8*, 99–115, 1989.

Stock, J. M., and K. V. Hodges, Miocene to Recent structural development of an extensional accommodation zone, northeastern Baja California, Mexico, *J. Struct. Geol.*, *12*, 315–328, 1990.

Taylor, B., A. Goodliffe, F. Martinez, and R. Hey, Continental rifting and initial sea-floor spreading in the Woodlark Basin, *Nature*, *374*, 534–537, 1995.

Taylor, B., A. M. Goodliffe, and F. Martinez, How continents break up: Insights from Papua New Guinea, *J. Geophys. Res.*, *104*, 7497–7512, 1999.

ten Brink, U. S., R. Katzman, and J. Lin, Three-dimensional models of deformation near strike-slip faults, *J. Geophys. Res.*, *101*, 16,205–16,220, 1996.

Teyssier, C., B. Tikoff, and M. Markley, Oblique plate motion and continental tectonics, *Geology*, *23*, 447–450, 1995.

Thatcher, W., and J. N. Brune, Seismic study of an oceanic ridge earthquake swarm in the Gulf of California, *Geophys. J. R. Astron. Soc.*, *22*, 473–489, 1971.

VanAndel, T. H., Recent marine sediments of Gulf of California, in *Marine Geology of the Gulf of California*, edited by T. van Andel and G. G. Shor, *AAPG Mem.*, *3*, 216–310, 1964.

Withjack, M. O., and W. R. Jamison, Deformation produced by oblique rifting, *Tectonophysics*, *126*, 99–124, 1986.

Woodcock, N. H., and M. Fischer, Strike-slip duplexes, *J. Struct. Geol.*, *8*, 725–735, 1986.

J. B. Diebold, G. S. Mountain, and M. S. Steckler, Lamont-Doherty Earth Observatory, Palisades, NY 10964, USA. (johnd@ldeo.columbia.edu; mountain@ldeo.columbia.edu; steckler@ldeo.columbia.edu)

A. González-Fernández and A. Martín-Barajas, CICESE, Km. 103 Carr. Tijuana-Ensenada, Ensenada Baja, California, C P 22830, Mexico. (mindundi@cicese.mx; amartin@cicese.mx)

P. Persaud and J. Stock, Seismological Lab, 252-21, California Institute of Technology, Pasadena, CA 91125, USA. (ppersaud@gps.caltech.edu; jstock@gps.caltech.edu)

Figure 1. (opposite) (a) Map of the Gulf of California. Heavy box outlines the survey area, which is shown in more detail in Figure 1b. Black arrows indicate the current Pacific-North America relative plate motion direction, N37°W [*Atwater and Stock*, 1998]. Pacific-North America plate boundary faults and spreading centers are from *Fenby and Gastil* [1991]. The major rift basins in the Gulf are labeled. (b) Location of multichannel seismic lines in the northern Gulf of California collected by the *Ulloa* in 1999. Stars mark sonobuoy locations. Seismic profiles shown in this work are marked with thick black lines and labeled. Arrowheads mark the right ends of the plotted seismic data. Lines 6 and 17 are shown in figures only. The rest of the seismic profiles are shown in foldouts, which refer to figures for more detail. ABF, Agua Blanca Fault; BTF, Ballenas Transform Fault Zone; CPF, Cerro Prieto Fault; CR, Consag Rock; EF, Elsinore Fault; EPR, East Pacific Rise; GB, Gonzaga Bay; IA, Isla Angel de la Guarda; IF = Imperial Fault; ISL = Isla San Luis; SAFZ, San Andreas Fault Zone; SJF, San Jacinto Fault; SB, Salsipuedes Basin; SMF, San Miguel Fault; SPMF, San Pedro Mártir Fault; ST, Salton Trough; TB, Tiburón Basin; TI, Tiburón Island; VP, Volcán Prieto. W1, W2, and W3 are PEMEX proprietary wells.

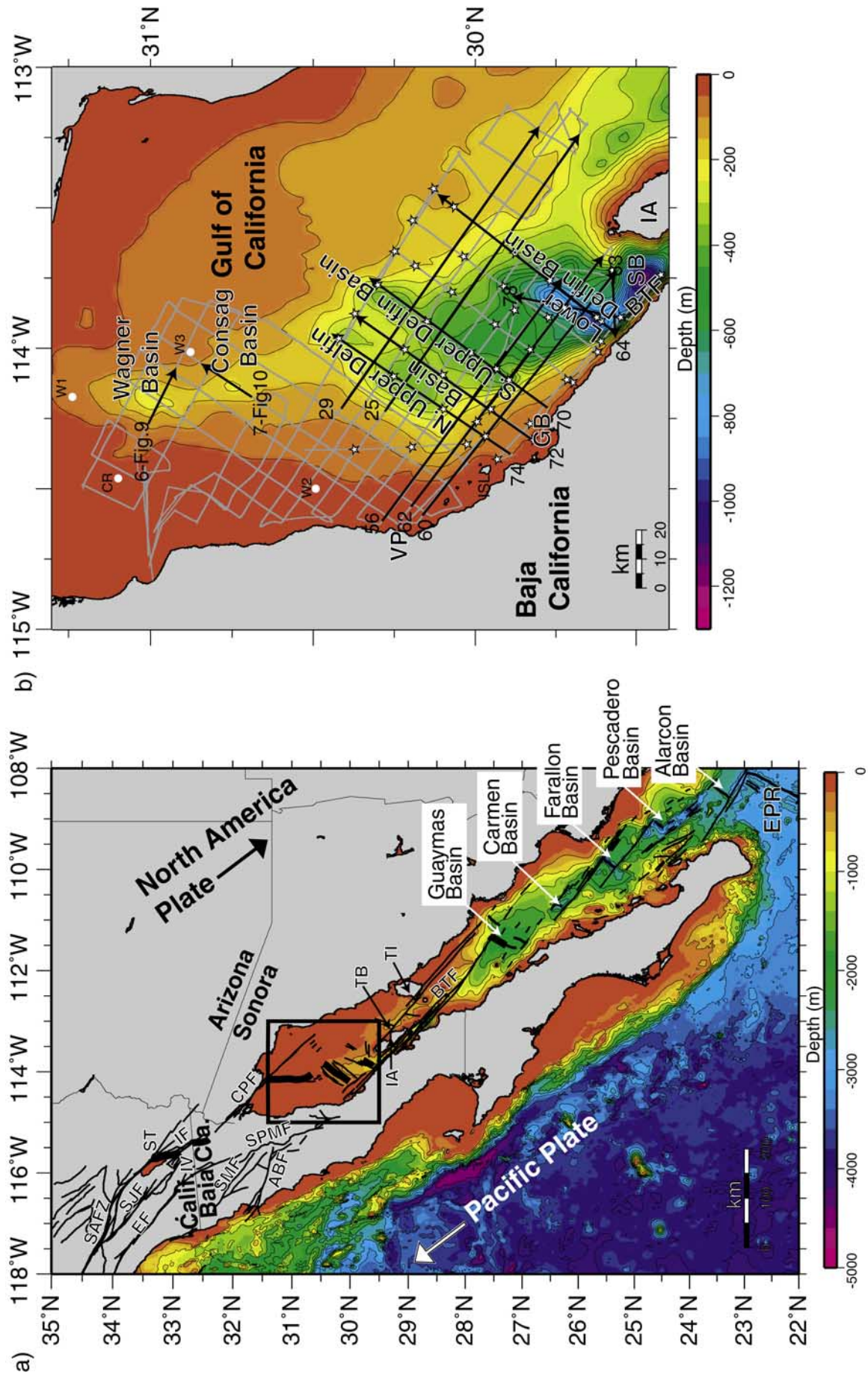
a)
b)
North America Plate
Pacific Plate
Arizona
Sonora
Baja Ca.
Calif.
Gulf of California
Baja California
Wagner Basin
Consag Basin
Upper Delfin Basin
N. Upper Delfin Basin
S. Upper Delfin Basin
Lower Delfin Basin
Guaymas Basin
Carmen Basin
Farallon Basin
Pescadero Basin
Alarcon Basin
EPR
SAFZ
SJF
EF
IF
ST
SMF
SPMF
ABF
CPF
TB
TI
BTF
IA
SB
GB
ISLI
VP
CR
W1
W2
W3
6-Fig.9
7-Fig10
Depth (m)
km

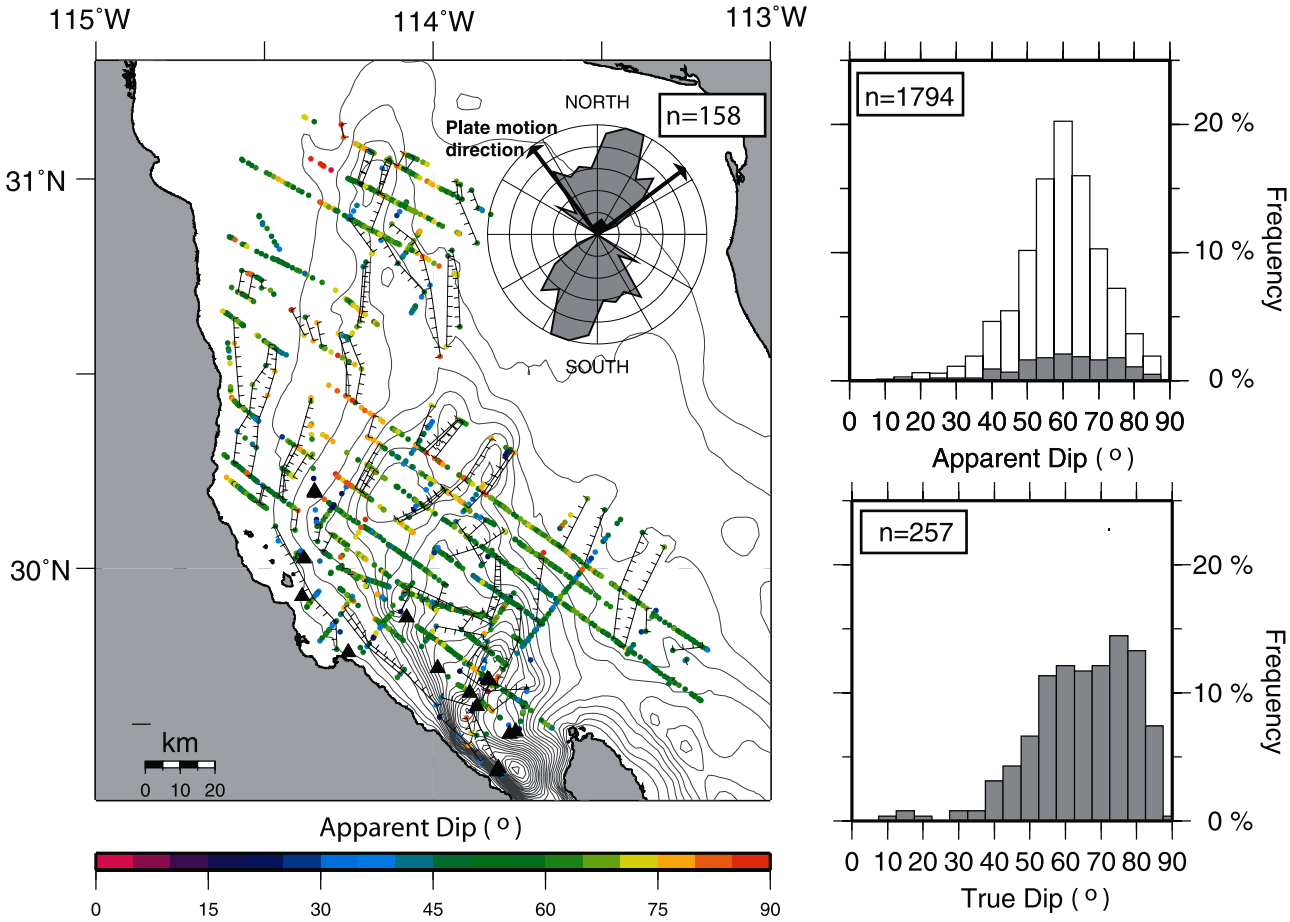

Figure 4. Map showing the apparent dips of all interpreted faults (total of 1794), calculated in the plane of the seismic profiles with a mean seismic velocity of 2000 m/s. Gray lines are bathymetric contours every 50 m. Strikes of all faults that were imaged on at least two seismic profiles (black lines) are shown in the inset rose diagram. This rose plot is normalized for equal area and shows a total of 158 fault segments or 112 faults with the maximum radius representing 24 fault segments. Note the approximate trends of the major rift basins are LDB = N10°E, NUDB and SUDB = N35°E and WB = N25°E (Figure 11). The dominant strike of faults in the survey area is N-N30°E, which is within 5–10° of the trend of the major rift basins. The top histogram shows the apparent dips of all faults; the gray shaded area represents the apparent dips of the faults shown by black lines in the map. The bottom histogram shows the true dip of these faults, which were calculated using the strikes.

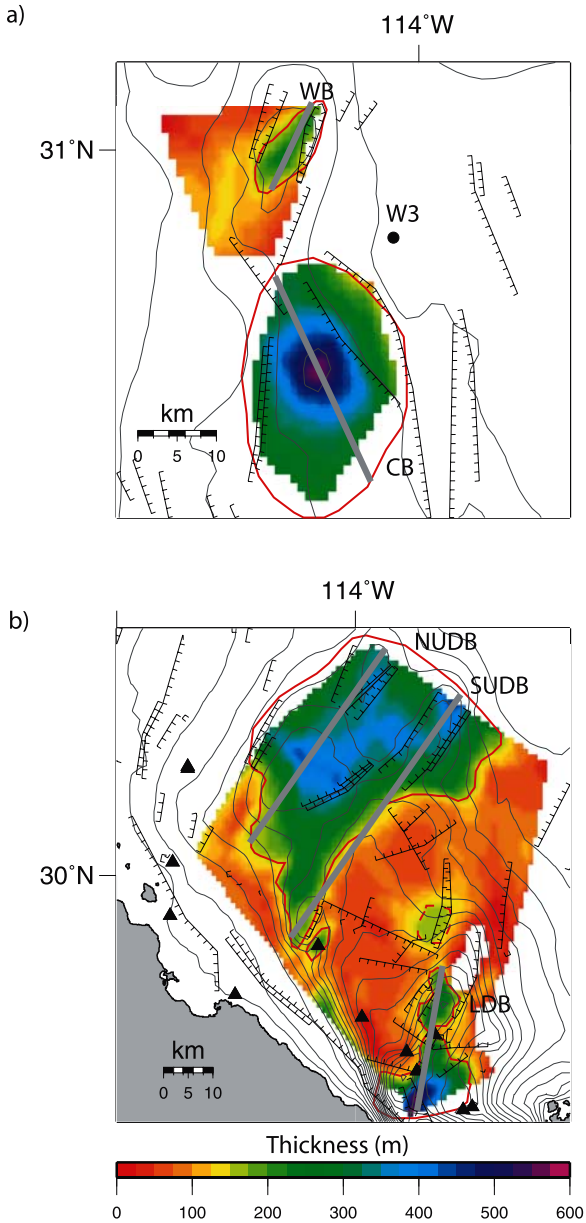

Figure 11. Isopach maps of the youngest sediments in (a) the Wagner and Consag Basins and (b) the Upper Delfín and Lower Delfín Basins. Thickness is given in meters below the seafloor. A velocity of 2000 m/s was used to convert TWTT to thickness. Solid red lines outline the major basins/depocenters. Thick gray lines represent the axes of the basins. These are based on the 150 m isopach. An additional small depocenter with no bathymetric expression is also shown (dashed red line). CB, Consag Basin; LDB, Lower Delfín Basin; NUDB, Northern Upper Delfín Basin; SUDB, Southern Upper Delfín Basin; W3, PEMEX well.

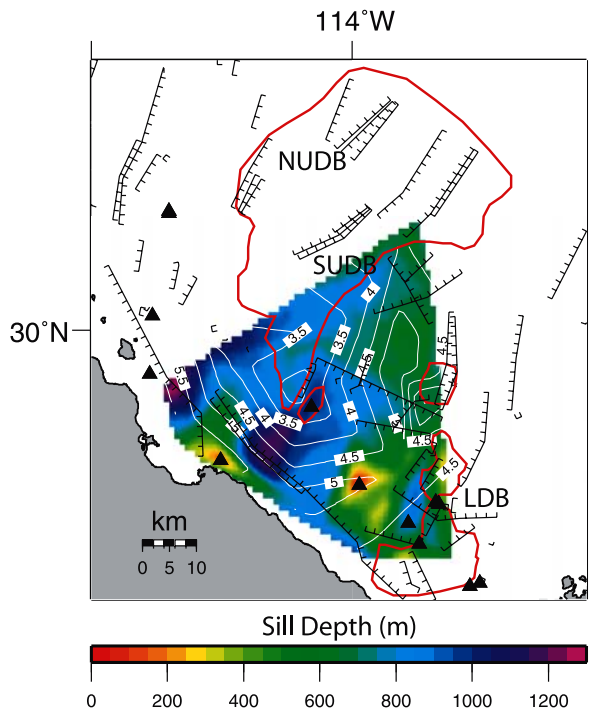

Figure 12. Map showing sill depth in meters below the seafloor overlain by contours (white lines) of *P* wave velocities at 2.8 km depth below the sea surface. Contours are shown at 0.5 km/s intervals. The sill depths shown are for multiple sills and represent an interpolation between different bodies. The major basins are outlined in red, based on the 150-m isopachs shown in Figure 11. Triangles are volcanic knolls.

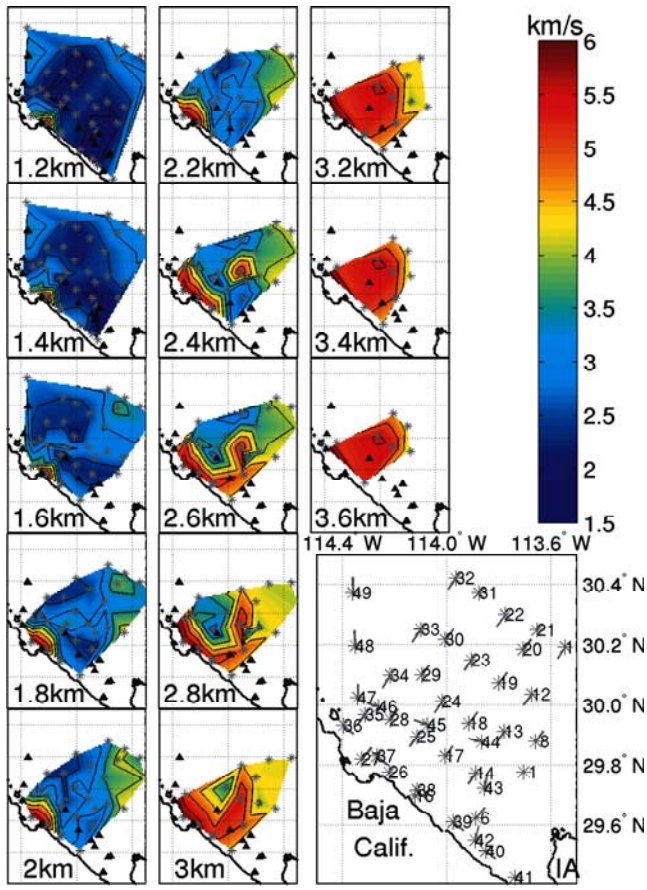

Figure 13. Depth slices showing interval velocities in the northern Gulf of California. Black triangles are volcanic knolls and gray stars mark the sonobuoy locations with tails pointing in the direction in which the ship was travelling. In each depth slice, the gray stars show the sonobuoys with data at that depth. IA, Isla Angel de la Guarda.